A general formulation for multi-modal dynamic traffic assignment considering multi-class vehicles, public transit and parking

Xidong Pi[a], Wei Ma[a], Zhen (Sean) Qian[a,b,*]

[a]Department of Civil and Environmental Engineering
Carnegie Mellon University, Pittsburgh, PA 15213
[b]Heinz College
Carnegie Mellon University, Pittsburgh, PA 15213

Abstract

Travel behavior and travel cost in modern urban transportation systems are impacted by many aspects including heterogeneous traffic (private cars, freight trucks, buses, etc.) on roads, parking availability near destinations, and travel modes available in the network, such as solo-driving, carpooling, ride-hailing, public transit, and park-and-ride. Managing such a complex multi-modal system requires a holistic modeling framework of transportation network flow in terms of both passenger flow and vehicular flow. In this paper, we formulate and solve for spatio-temporal passenger and vehicular flows in a general multi-modal network explicitly considering multi-class vehicles, parking facilities, and various travel modes. Vehicular flows, namely cars, trucks, and buses, are integrated into a holistic dynamic network loading (DNL) models. Travel behavior of passenger demand on modes and routes choices is encapsulated by a multi-layer nested logit model. We formulate the multi-modal dynamic user equilibrium (MMDUE) that can be cast into a Variational Inequality (VI) problem. A simple flow solution performed at the origin-destination level and based on the gradient projection is derived from the KKT conditions and shown to efficiently solve for the VI problem on large-scale networks. Numerical experiments are conducted on a multi-modal network in the Pittsburgh region along with sensitivity analysis with respect to demand and management strategies. We show that many factors including the total passenger demand, parking prices, transit fare, and ride-sharing impedance can effectively impact the system performance and individual user costs. Experiments on a large-scale multi-modal network in Fresno, California also show our model and solution algorithms have satisfactory convergence performance and computational efficiency.

Keywords: multi-modal dynamic user equilibrium, nested logit model, dynamic traffic assignment, heterogeneous traffic simulation, public transit, parking

1. Introduction

Thanks to cutting-edge communication and sensing technologies, new transportation modes are emerging while traditional modes are also being improved and innovated through technologies. Vehicles and rides can be shared from end to end, such as pick up, drop off, and parking. Transportation becomes unprecedentedly ubiquitous, low cost and diversified nowadays, especially in densely populated metropolitan areas. People frequently take public transit (subway, regular bus, first/last mile feeder transit, paratransit, etc.), carpool, or use the ride-hailing services like taxis, Uber and Lyft, in addition to driving in a private car. To make modal choices, travelers make trade-offs among traffic congestion, convenience, parking fare, parking cruising time, and expenditures to pay for travel. From the system perspective, the co-existence of all these travel modes leads to diversified and complex systems that enable more instruments to alleviate traffic congestion and improve users' quality of life, provided that the comprehensive system of systems can be designed, modeled and operated effectively. In this research, we formulate and solve for spatio-temporal passenger and vehicular flows in a general multi-modal network explicitly considering multi-class vehicles (private cars, freight trucks, buses, etc.), parking facilities and various travel modes

---

*Corresponding author
Email addresses: xpi@cmu.edu (Xidong Pi), weima@cmu.edu (Wei Ma), seanqian@cmu.edu (Zhen (Sean) Qian)

including solo-driving, carpooling, ride-hailing, bus transit, railway transit, parking, and park-n-ride. The intention is to develop a general mathematical formulation to comprehensively model the entire transportation system that would allow the flexibility of modeling any subset of vehicles, passengers and modes. Insights are provided to better understand the interaction and linkage among each component of the transportation system and to ultimately facilitate optimal decision making on holistic system planning and operation.

In general, given the transportation network supply and Origin-Destination (OD) demand, a dynamic traffic assignment (DTA) allocates the spatio-temporal flow of both vehicles and passengers on the network with a pre-determined behavioral model (oftentimes the choices of routes, departure time and modes). In a multi-modal transportation network that integrates roadways, public transit, and parking, multi-modal DTA yields the performance of each mode of transportation systems in terms of spatio-temporal flow. Over the last few decades, DTA with a single travel mode of solo-driving has been studied intensively. Travelers' behavior in choosing different traffic modes altogether, such as the public transit, carpooling, park-and-ride (PnR), as well as travelers' behavior related to parking, were not the focus of the conventional DTA problem. On the other hand, simulation-based DTA on large-scale networks requires dynamic network loading (DNL) models to obtain travel costs/time. Most of existing DNL models assume homogeneous traffic flow in the unit of standard passenger cars, e.g., a single-class cell transmission model (Daganzo 1994). Multiple vehicle classes, such as buses, trucks and standard passenger cars, can be explicitly modeled in DNL, but are usually not explicitly considered when augmenting the DNL with behavior models in a DTA model. Another challenge for DTA is how to make the best use of the spatio-temporal data for different travel modes to best understand travel patterns and connections across those modes and to validate DTA models. In this paper, we proposed a general formulation of multi-modal dynamic user equilibrium (MMDUE) problem considering both the travelers' behavior across multiple modes and heterogeneous traffic flow in multi-modal networks. This general framework that holistically models many components of a transportation system would enable further validation by emerging real-world data collected from roadway, public transit, and parking systems. Though this paper does not focus on validation using real-world data, we show that the holistic model holds great promises to quantify ripple effects of disruption to any part of a transportation network, and thus is able to provide policy/managerial insights.

In the literature, although the private driving mode was studied the most, the multi-modal network modeling still received adequate attention in the past, mostly in static network settings. Early in the 1970s, Wigan & Bamford (1973) and Florian (1977) studied traffic network equilibrium modeling with the consideration of traveling by cars and buses. Florian (1977) combined demand functions for each mode of travel, route choice equilibrium conditions, transit network models and the interactions of different classes of vehicles on the links on an integrated network simultaneously. Abdulaal & LeBlanc (1979) presented a combined modal split and assignment model which allows choosing traveling modes and routes simultaneously, with its extension (Leblanc & Abdulaal 1982) to multi-class users where trip distribution, modal split, and traffic assignment are all combined simultaneously. Similarly, a number of other works also advanced the formulation, analysis, and algorithms of multi-modal network equilibrium problems (Dafermos 1982, Florian & Spiess 1983, Lam & Huang 1992). These studies often considered two or three traffic modes (mostly private car, public transit) and represented travel time/cost as a single link-based cost function due to the nature of a static network.

In addition to the aforementioned studies considering "plain" mode of travel, there are also plenty of studies in which the "composite" or "combined" mode is explicitly presented, for example, the park-and-ride or bus/ride-hailing access to metro. Florian & Los (1979) proposed a model for determining the intermediate OD matrices from trip origins to parking lots and from parking lots to final destinations for park-and-ride travelers using Lindenwold rapid transit line in Philadelphia. Fernández et al. (1994) gave a classic steady-state assignment model that combines the binary mode choice and passenger flow assignment. They assumed that the probability of choosing a traffic mode follows a logit model. Lo et al. (2003) studied the modeling of transfers in multi-modal networks, which involves "combined mode" trips. It explicitly considered the number and types of transfers, and it also accommodated a non-linear fare structure, which was extended by Lo et al. (2004). In Garcia & Marin (2005), users' mode choice and transfer location choice are governed by a nested logit model, and the static user equilibrium is formulated as a variational inequality (VI) problem, which is solved by a disaggregate simplicial decomposition algorithm. These studies are not conducted in the "dynamic" network setting, hence the dynamic evolution of demand and congestion was not considered.

More recently, Abdelghany & Mahmassani (2001) proposed a simulation-based DTA model with several travel modes including private cars, buses, metro-subway, and carpooling. A medium-sized network experiment was pre-

sented with no parking facility and parking cruising behavior explicitly modeled in the simulation. This work was extended in Zhou et al. (2008) to be applied to a large-scale multi-modal network from the Baltimore-Washington corridor, but parking behaviors and heterogeneous traffic (cars, trucks, buses, etc.) are still not considered. Zhang, Nair, Mahmassani, Miller-Hooks, Arcot, Kuo, Dong & Lu (2008) studied the dynamic freight assignment problem on a large-scale inter-modal network in Europe. In this study, they used a dynamic micro-assignment method to make a joint mode, path, service, and carrier choice. Verbas et al. (2015) studied the dynamic assignment-simulation methods in large-scale urban multi-modal transit networks, with the assumption that link travel times of transit vehicles are independent of traffic network conditions. In Zheng & Geroliminis (2016) and Zheng et al. (2016), the modeling and optimization of multi-modal networks with parking space limitation and dynamic parking pricing were studied based on the macroscopic fundamental diagram (MFD). Chiabaut (2015) extended MFD to passenger based MFD which combines several modes. Meschini et al. (2007) proposed a bi-modal DTA model with private cars and public transit, and solved for equilibrium solutions using a macroscopic flow model without a DNL process. Liu & Geroliminis (2017) presented a multi-region multi-modal transportation system model that enables travelers to update their travel patterns on a day-to-day basis, based on which an adaptive parking pricing strategy can be proposed to effectively reduce the total social cost. Other modeling approaches including activity-based model are also intensively studied for the past decade, for example, MATSIM (Axhausen et al. 2008, Horni et al. 2016) is an agent-based simulation tool for multi-modal transportation networks. However, it requires a large amount of survey data about urban residents' daily activities and schedules to build the activity chains of residents as the input of the model, which is usually costly to obtain. In MATSIM, the DUE is solved by iteratively re-planning each individual's daily activity chains, which makes it hard to calibrate the model and validate the results for large-scale networks. The reasons are: 1) individuals daily activity data are hard to acquire; 2) calibrating an activity-based model in the network level using large-scale activity data and traffic data (e.g. counts/speeds) are very challenging. The computational challenge for large-scale network is another issue. Simulation and traffic analysis platforms, e.g., VISUM-VISSIM (PTV 2018), can also provide realistic multi-modal traffic simulation features. However, the DUE can only be solved for private traffic in VISUM without public transportation and parking behavior. Other open-source DTA tools like DTALite (Zhou & Taylor 2014), DTALite-S (Tong et al. 2019), etc. also consider multi-modal traffic including driving and public transportation, but other travel modes and parking behavior are not explicitly modeled. To our best knowledge, research gap exists where large-scale multi-modal DTA explicitly integrates passenger flow and vehicular flow, and holistically considers heterogeneous traffic flow on roads, traveler's parking behaviors, and various travel modes including solo-driving, carpooling, ride-hailing, bus transit, railway transit, and park-and-ride. Complications are to integrate realistic behavioral models as well as network flow models in such a general and complex multi-modal network, and to solve such a complex network model efficiently and effectively that can be calibrated with large-scale transportation data.

In this paper, we establish a general multi-modal dynamic user equilibrium (MMDUE). It is capable of modeling four travel modes, driving (including solo-driving and carpooling), ride-hailing, public transit (including railway with its own right-of-way and buses that share the roadway with private vehicles), and park-and-ride. It is also capable of modeling travelers' parking behavior (including parking lot choice and parking cruising time). Travelers choose their travel modes and routes with respect to their generalized travel costs of all options made available to them. A multi-modal DNL model simulates multi-class vehicles (cars, trucks, and buses) to estimate travel costs by mode and by route. MMDUE is then solved in the multi-modal multi-class network using a newly developed gradient projection algorithm that possesses a simple form and is efficient for large networks. System performance and features of passenger/vehicular flow can then be assessed for decision making.

This research makes the following major contributions to the literature:

- It establishes a combined multi-modal transportation network consisting of an auto network, a railway network, a bus network, and parking facilities. This combined network allows modeling of vehicular and passenger flow, composite modes through paths in the network, as well as link and path-based generalized travel cost for passengers.

- It explicitly considers parking choices over time. Choices of parking near destination and park-and-ride stations are dependent on parking prices and parking cruising time.

- It proposes a new MMDUE formulation across all possible modes, such as solo-driving, carpooling, ride-hailing, bus transit, railway transit, and park-and-ride. Mode choices are governed through a multi-layer

nested logit model. A novel VI formulation and its equivalence to the MMDUE is provided and shown.

- The multi-modal DNL process is capable of modeling the propagation of mixed traffic flow including cars, trucks, and buses.

- It solves the VI formulation for MMDUE with a new projection based solution algorithm. The algorithm is performed at the O-D level, and thus can be efficient in terms of computational time and storage. It shows decent convergence performance compared to existing algorithms.

- The proposed model and algorithm can help understand the comprehensive interaction and linkage among each component of complex transportation systems. The case study demonstrates how to quantify such a "ripple effect" to the comprehensive system induced by interventions on demand, supply, and management strategies.

The content of this paper is arranged as follows. Section 2 first introduces the combined multi-modal transportation network and illustrates the difference between passenger/vehicle path, flow, and demand with an illustrative example. Section 3 describes the mode choice model of travelers in the general multi-modal traffic systems and formulates the MMDUE problem as a discrete VI problem. Then section 4 describes the mesoscopic multi-modal DNL model used in the simulation and how to use simulation for estimation of travel costs. Section 5 provides the algorithm to solve the VI problem, hence to obtain the user equilibrium state of the multi-modal system. In section 6, we show the performance of our model and algorithm on two multi-modal networks of Pittsburgh, PA and Fresno, CA, with roadway driving, public transit, and parking. The convergence property and equilibrium solution are thoroughly analyzed. Multiple sensitivity analyses are also performed to show the properties and stability of the multi-modal traffic system. Section 7 concludes this paper. The main notations used in this paper are listed in Table A.4 in Appendix A.

2. A Combined Multi-modal Transportation Network

This paper first establishes a combined multi-modal transportation network consisting of an auto network, a railway network, a virtual bus network and parking facilities. Buses share the same roadway network as cars, and therefore a virtual bus network is created by combining a copy of part of the roadway network and bus stations (as shown in Figure 1). A physical stop (PS) is a bus stop where bus passengers board/alight the buses, and it can be associated with multiple routes. On the other hand, a virtual stop (VS) connects a PS to a particular route, and it does not physically exist. The link between any two VSes describes the movement of a bus between the two corresponding PSes on a particular route. While a bus follows a fixed route in the virtual bus network, its travel cost/time is modeled by the DNL model with multiple classes of vehicles, e.g. private cars, trucks, and buses, in the auto network. The railway transit routes have their own right-of-way and therefore are separated from the auto network. Similar to bus transit, we also used physical railway station (PR) and virtual railway station (VR) and the boarding/alighting links to model the passenger waiting at stations, boarding and alighting from railway trains. Also, there are two types of parking facilities considered in the network, park-and-ride stations, and near-destination parking lots/spaces. If travelers commute from the suburban area to the central business district (CBD), they have choices of parking their cars at one of those park-and-ride stations along the corridor and then take the transit to the destination, which is represented by the parking (P) nodes in Figure 1 and it requires an additional transfer time between the driving mode and transit mode. Or if they choose to drive all the way to the CBD, then they need to park near their destinations and usually pay for high parking fees. Another choice is to use the ride-hailing service, which requires a ride fee but exempts from time finding a parking space as well as paying the parking fee. In this multi-modal network, walking links are also explicitly modeled to represent walking from origin to bus stops and train stations, from the parking area to bus stops and train stations, transfer among bus stops and train stations, and from parking areas, bus stops and train stations to the final destination.

Note in this multi-modal network, the path, flow and demand of passengers are different from those of vehicles. A passenger path is retrieved on the multi-modal network with the auto network, virtual bus network, railway network and parking facilities all combined. Thus, between any origin and destination (OD) there could be multiple paths under different travel modes. But for a vehicle path, railway train and buses follow the fixed paths, while a private car's path is just a portion of a passenger's path on the auto network (e.g. the driving portion of a park-n-ride

path). The vehicle demand between any OD is dependent on the passenger demand as well as their mode choices. Different classes of vehicles are generated and loaded on the network and they can also carry different numbers of passengers. Example 1 shows the difference between passenger and vehicle flow.
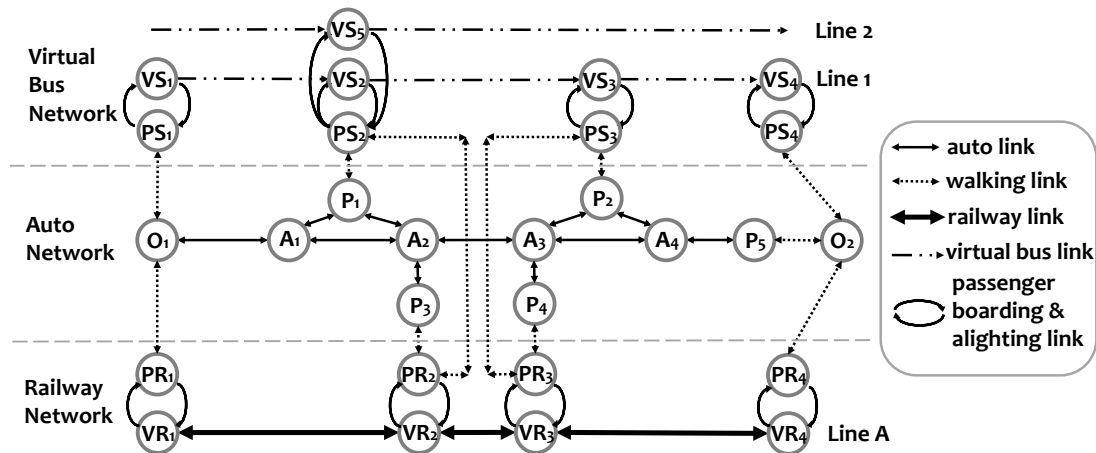

Figure 1: A combined multi-modal transportation network: O: OD node; A: auto node; P: parking node; PS: physical bus stop; VS: virtual bus stop; PR: physical railway station; VR: virtual railway station.

Example 1 (Passenger/vehicle path, flow and demand). *In this example, we illustrate the differences between passenger/vehicle flow. In Figure 1, we study the passenger demand $q_t^{O_1 O_2}$ for OD pair (O_1, O_2) at time t. Suppose $q_t^{O_1 O_2} = 10$, we consider three passenger paths at time t as follows:*

- *Two passenger carpool, $O_1 \rightarrow A_1 \rightarrow A_2 \rightarrow A_3 \rightarrow A_4 \rightarrow P_5 \rightarrow O_2$, passenger flow 6*

- *Park-and-ride, $O_1 \rightarrow A_1 \rightarrow P_1 \rightarrow PS_2 \rightarrow VS_2 \rightarrow VS_3 \rightarrow VS_4 \rightarrow PS_4 \rightarrow O_2$, passenger flow 3*

- *Railway, $O_1 \rightarrow PR_1 \rightarrow VR_1 \rightarrow VR_2 \rightarrow VR_3 \rightarrow VR_4 \rightarrow PR_4 \rightarrow O_2$, passenger flow 1*

For example, $O_1 \rightarrow A_1$, $A_i \rightarrow A_{i+1}, i = 1, 2, 3$ and $A_1 \rightarrow P_1$ refer to the link travel by car, $P_1 \rightarrow PS_2$ refers to walking from the parking lot to bus station, $PS_2 \rightarrow VS_2$ refers to bus boarding, $VS_i \rightarrow VS_{i+1}, i = 1, 2, 3$ refer to the link travel by bus, VS_4 to PS_4 refers to bus alighting and $PS_4 \rightarrow O_2$ refers to walking from bus stop to destination. Similarly, $VR_i \rightarrow VR_{i+1}, i = 1, 2, 3$ refer to the railway travel.
We formulate the corresponding vehicle flow as follows:

- *Car (two passenger carpool), $O_1 \rightarrow A_1 \rightarrow A_2 \rightarrow A_3 \rightarrow A_4 \rightarrow O_2$, vehicle flow $6/2 = 3$*

- *Car (park-and-ride), $O_1 \rightarrow A_1 \rightarrow P_1$, vehicle flow 3*

- *Bus (Line 1), this vehicle path is pre-determined by the public transit operator, and the vehicle flow is independent of passenger flow, but relates to the bus schedule*

In this study, vehicular flow is explicitly simulated on the auto network, for estimating the dynamic network conditions including the traffic states on links and at intersections, as well as the parking occupancy in parking facilities. Passenger flow is not loaded on the network but is fulfilled by the vehicle loading process under the constraint of network demand and supply. In detail, given passenger OD demand, their mode choice and route choice models yield the passenger path/flow based on initial network conditions. We then calculate the vehicle flow from passenger path/flow and their mode choices, and load vehicles on the network and update the network conditions. The mode and route choices can be updated based on new network conditions, so do the passenger flow and vehicle flow. This procedure goes on until the equilibrium state is achieved. The whole process is shown in Figure 2.
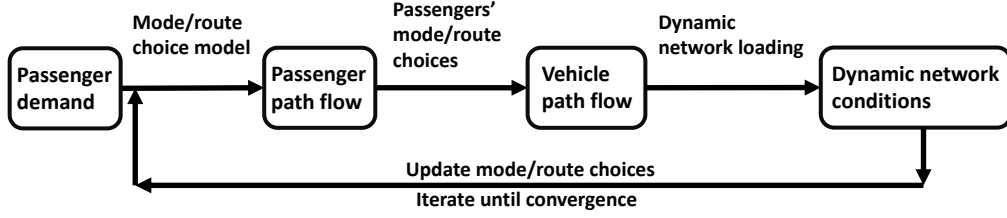
Figure 2: The whole process for solving MMDUE in this study.

3. Mode Choice and Network Equilibrium

3.1. A nested-logit mode choice model

In this research, mode choices are determined by a nested logit model shown in Figure 3. For any O-D pair, in the upper level, travelers choose to drive, use ride-hailing service, take the transit or use a combined mode (park-and-ride). For travelers who choose to drive, they have the choices of either driving alone or carpool with others in the lower decision level. For travelers who choose to use ride-hailing service, they have the choices of either ride-hailing all the way to the destination or ride-hailing to any railway station and then transfer to the railway mode. If travelers choose public transit, then they can take the bus, railway train or transfer between both bus and railway mode. If they choose a combined mode, then there are four choices in their lower decision level including solo-driving + bus, solo-driving + railway, carpooling + bus, carpooling + railway.
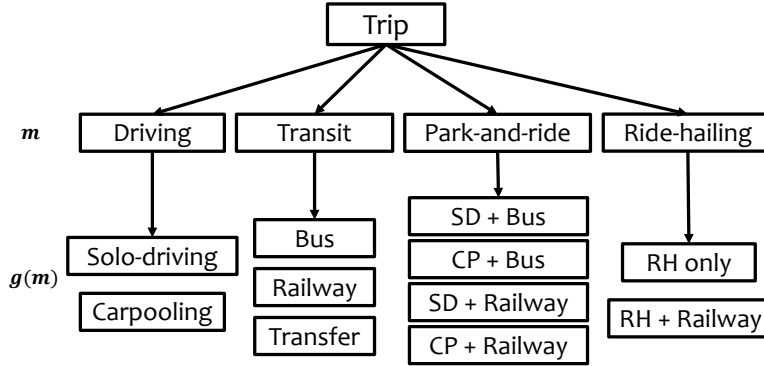

Figure 3: The two-layer mode choices ("SD" = "solo-driving", "CP" = "carpooling", "RH" = "ride-hailing")

Following the work of Arnott et al. (1990) and Qian & Zhang (2011), we define the generalized traveling cost for each travel mode. We use the subscripts 1, 2, 3 and 4 to represent the transit mode, driving mode, ride-hailing mode and park-and-ride mode, respectively. Let $c_{m,k,t}^{rs}$, $m \in \{1, 2, 3, 4\}$ denote the generalized travel cost of a traveler from r to s using travel mode m departing at time t and taking the path k, $\forall k \in P_m^{rs}$, where P_m^{rs} denote the path set for mode m from r to s. A transit passenger is subject to the following generalized travel cost $c_{1,k,t}^{rs}$,

$$c_{1,k,t}^{rs} = \alpha w_{k,t}^{rs} + max[\gamma(t + w_{k,t}^{rs} - t^*), \beta(t^* - t - w_{k,t}^{rs})] + \delta_k^{rs} + \sigma_{k,t}^{rs}, \ \forall k \in P_1^{rs} \tag{1}$$

where:

- $w_{k,t}^{rs}$ denotes the actual travel time through path k at time t from r to s, note in this case the actual travel time $w_{k,t}^{rs}$ is the summation of possible transit waiting time, bus/railway travel time and all possible walking time, including from origin to transit station, transfer among transit stations, and from transit station to destination, during this trip.

- t^* is the standard work starting time. α is the unit cost of travel time. γ and β are the unit cost of time for arriving late and arriving early, respectively. This second term is known as the schedule delay cost.

6

- δ_k^{rs} represents the transit fare of transit route k from r to s.

- $\sigma_{k,t}^{rs}$ is the possible perceived inconvenience cost of the transit mode associated with the crowding of transit route k from r to s.

As indicated by previous models of dynamic transit network, e.g. Liu & Zhou (2016), the vehicle carrying capacity of public transportation could be an important constraint that affects travelers' choice of using public transportation under certain circumstances, for example when the public transit vehicle is highly crowded and the service is unreliable. We can explicitly or implicitly model the vehicle capacity during the dynamic public transit loading. The vehicle capacity can be strictly enforced by maintaining a passenger flow queue at each physical transit stop and adding passenger flow to transit vehicles only if the in-vehicle flow does not exceed the capacity. In addition, the capacity constraints can be implicitly incorporated in the perceived inconvenience cost $\sigma_{k,t}^{rs}$. For different public transit lines the inconvenience costs can be estimated based on the historical data of crowding level, on-time performance, etc. Transit lines with high crowding level and poor on-time performance will cause larger perceived inconvenience cost $\sigma_{k,t}^{rs}$.

Similarly, if we assume carpooling is only available for travelers with same origins and destinations, then the pick-up and drop-off travel time can be ignored. Then the generalized travel cost of driving departing at time t and taking the path k is,

$$c_{2,k,t}^{rs} = \alpha w_{k,t}^{rs} + max[\gamma(t + w_{k,t}^{rs} - t^*), \beta(t^* - t - w_{k,t}^{rs})] + \frac{p_i}{n} + \Delta_{k,t}^{rs}(n) + \xi, \ \forall k \in P_2^{rs} \tag{2}$$

Where:

- p_i is the parking fee at parking area i, here parking area i is on the path k.

- n is the number of pooled travelers, and $n = 1$ means solo-driving. $\Delta_{k,t}^{rs}(n)$ represents the carpooling impedance cost through path k at time t from r to s with total n riders, $\Delta_{k,t}^{rs}(1) = 0$.

- ξ is an indicator of accessibility to a private car. If the traveler owns a car or has access to a private car then $\xi = 0$, otherwise it should be a large constant.

- For achieving a higher model fidelity, the fuel costs and vehicle depreciation can also be included to the cost function. Here we omit these costs to simplify the calculation in numerical experiments.

The generalized travel cost of using ride-hailing service departing at time t and taking the path k is,

$$c_{3,k,t}^{rs} = \alpha w_{k,t}^{rs} + max[\gamma(t + w_{k,t}^{rs} - t^*), \beta(t^* - t - w_{k,t}^{rs})] + \rho_{k,t}^{rs}, \ \forall k \in P_3^{rs} \tag{3}$$

Where $\rho_{k,t}^{rs}$ is the ride fee of the ride-hailing service through path k at time t from r to s. Here $w_{k,t}^{rs}$ should also include waiting time for pick up in addition to the car travel time.

The generalized travel cost of park-and-ride departing at time t and taking the path k is,

$$c_{4,k,t}^{rs} = \alpha w_{k,t}^{rs} + max[\gamma(t + w_{k,t}^{rs} - t^*), \beta(t^* - t - w_{k,t}^{rs})] + \frac{p_i}{n} + \Delta_{k,t}^{rs}(n) + \delta_k^{rs} + \sigma_{k,t}^{rs} + \xi, \ \forall k \in P_4^{rs} \tag{4}$$

A reasonable assumption is that parking is much cheaper at park-and-ride stations than near CBD. As a result, people usually park in the suburb and transfer to public transit to get to CBD. Note in this case the actual travel cost $w_{k,t}^{rs}$ is the summation of driving time, possible parking cruising time, walking time from parking lot to bus station, bus travel time and possible walking time from the station to the destination. We will discuss how to use dynamic network loading for computing $w_{k,t}^{rs}$ in Section 4.

3.2. Multi-modal dynamic user equilibrium (MMDUE)

The MMDUE with a nested logit mode choice model can be further formulated as a variational inequality (VI) problem. In particular, for formulating and solving the MMDUE in a more applicable way, the OD demand for each time interval t is assumed to be fixed, so there is no departure time choice in this paper. However, it is easy to extend MMDUE to accommodate departure time choice by relaxing the feasibility set.

Consider a single-level logit model applied in the dynamic multi-modal transportation network. The UE condition of the whole network reads, $\forall r, s, t, m$,

$$
\begin{aligned}
c_{m,k,t}^{rs} - \mu_{m,t}^{rs} &= 0 \quad \text{if } \forall k \in P_m^{rs}, f_{m,k,t}^{rs} > 0 \\
c_{m,k,t}^{rs} - \mu_{m,t}^{rs} &\geq 0 \quad \text{if } \forall k \in P_m^{rs}, f_{m,k,t}^{rs} = 0 \\
\frac{h_{m,t}^{rs}}{q_t^{rs}} &= \frac{e^{-(\alpha^m + \beta_1 \mu_{m,t}^{rs})}}{\sum_{m'} e^{-(\alpha^{m'} + \beta_1 \mu_{m',t}^{rs})}}
\end{aligned}
\tag{5}
$$

where $\mu_{m,t}^{rs}$ is the equilibrium cost of travel mode m from r to s departing at time t. $f_{m,k,t}^{rs}$ is the flow of path k in mode m from r to s departing at time t. The flow of mode m between O-D pair rs departing at time t is $h_{m,t}^{rs} = \sum_{k \in P_m^{rs}} f_{m,k,t}^{rs}$. The total flow between O-D pair rs departing at time t is $q_t^{rs} = \sum_{m \in \{1,2,3,4\}} h_{m,t}^{rs}$. The α^m and β_1 are parameters in the logit model.

Let $\mathbf{f}$ be the vector of all path flows. The MMDUE can be cast into a VI problem $\mathbf{VI}(\Lambda_1, \Omega_1)$ as follows (see proof in Section 3.3.1).

$$
\begin{aligned}
\text{Find } \mathbf{f}^* \text{ such that} \quad & \Lambda_1(\mathbf{f}^*)^T \cdot \ (\mathbf{f} - \mathbf{f}^*) \geq 0, \ \forall \mathbf{f} \in \Omega_1 \\
\text{where} \quad & \Lambda_1(\mathbf{f}) = \{\Lambda_{k,t}^{rs}(\mathbf{f})\} \\
& \Lambda_{k,t}^{rs}(\mathbf{f}) = c_{m,k,t}^{rs}(\mathbf{f}) + \frac{\alpha^m + \ln h_{m,t}^{rs}}{\beta_1} \\
& \Omega_1 = \{\mathbf{f} | \sum_k f_{m,k,t}^{rs} = q_t^{rs}\}
\end{aligned}
\tag{6}
$$

For a more general case where we have two levels of mode choices (a nested logit), let $g(m)$ denote the second level mode choices under first level mode choice m, and define the c, μ, P, f, q as same as the first-layer MMDUE. The two-layer MMDUE condition reads, $\forall r, s, t, m, g(m)$,

$$
\begin{aligned}
c_{m,g(m),k,t}^{rs} - \mu_{m,g(m),t}^{rs} &= 0 \quad \text{if } \forall k \in P_{m,g(m)}^{rs}, f_{m,g(m),k,t}^{rs} > 0 \\
c_{m,g(m),k,t}^{rs} - \mu_{m,g(m),t}^{rs} &\geq 0 \quad \text{if } \forall k \in P_{m,g(m)}^{rs}, f_{m,g(m),k,t}^{rs} = 0
\end{aligned}
$$

$$
\begin{aligned}
\frac{h_{m,t}^{rs}}{q_t^{rs}} &= \frac{e^{-(\alpha^m + \beta_1 \mu_{m,t}^{rs})}}{\sum_{m'} e^{-(\alpha^{m'} + \beta_1 \mu_{m',t}^{rs})}} \\
\frac{h_{m,g(m),t}^{rs}}{h_{m,t}^{rs}} &= \frac{e^{-(\alpha_{g(m)}^m + \beta_2^m \mu_{m,g(m),t}^{rs})}}{\sum_{g' \in G(m)} e^{-(\alpha_{g'}^m + \beta_2^m \mu_{m,g',t}^{rs})}} \\
\mu_{m,t}^{rs} &= -\frac{1}{\beta_2^m} \ln \left(\sum_{g' \in G(m)} e^{-(\alpha_{g'}^m + \beta_2^m \mu_{m,g',t}^{rs})} \right)
\end{aligned}
\tag{7}
$$

where $G(m)$ is the set of all second level mode choices under mode m. The $\alpha_{g(m)}^m$ and β_2^m are also parameters in the logit model. Note the last formula in (7) defines the relationship between the first level mode equilibrium cost $\mu_{m,t}^{rs}$ and the two levels mode equilibrium costs $\mu_{m,g(m),t}^{rs}$, $\forall g(m) \in G(m)$. In this case, the $\mu_{m,t}^{rs}$ is defined as an average over $\mu_{m,g(m),t}^{rs}$, $\forall g(m) \in G(m)$. The flow of mode $\{m, g(m)\}$ between O-D pair rs departing at time t is:

$$
\begin{aligned}
h_{m,g(m),t}^{rs} &= \sum_{k \in P_{m,g(m)}^{rs}} f_{m,g(m),k,t}^{rs} \\
h_{m,t}^{rs} &= \sum_{g(m) \in G(m)} \sum_{k \in P_{m,g(m)}^{rs}} f_{m,g(m),k,t}^{rs} = \sum_{g(m) \in G(m)} h_{m,g(m),t}^{rs}
\end{aligned}
\tag{8}
$$

It can also be cast into a VI problem $\mathbf{VI}(\Lambda_2, \Omega_2)$ as follows (see proof in Section 3.3.2).

$$
\begin{aligned}
\text{Find } \mathbf{f}^* \text{ such that} \quad & \Lambda_2(\mathbf{f}^*)^T \cdot \ (\mathbf{f} - \mathbf{f}^*) \geq 0, \ \forall \mathbf{f} \in \Omega_2 \\
\text{where} \quad & \Lambda_2(\mathbf{f}) = \{\Lambda_{m,g(m),k,t}^{rs}(\mathbf{f})\} \\
& \Lambda_{m,g(m),k,t}^{rs}(\mathbf{f}) = c_{m,g(m),k,t}^{rs}(\mathbf{f}) + \frac{\alpha^m + \ln h_{m,t}^{rs}}{\beta_1} - \frac{\ln h_{m,t}^{rs}}{\beta_2^m} + \frac{\alpha_{g(m)}^m + \ln h_{m,g(m),t}^{rs}}{\beta_2^m} \\
& \Omega_2 = \{\mathbf{f} | \sum_m \sum_{g(m)} \sum_k f_{m,g(m),k,t}^{rs} = q_t^{rs}\}
\end{aligned}
\tag{9}
$$

3.3. Proof of VI formulations equivalent to MMDUE

Proposition 3.3 (*Nagurney 2009*): *Let $F : \mathbb{R}^n \mapsto \mathbb{R}^n$ and $\mathbb{R}_+^n$ denote the nonnegative orthant in $\mathbb{R}^n$. The following complementarity problem:*

$$
\text{Find } \mathbf{x}^* \geq \mathbf{0} \text{ such that } \Lambda(\mathbf{x}^*) \geq \mathbf{0} \text{ and } \Lambda(\mathbf{x}^*)^T \mathbf{x}^* = 0
\tag{10}
$$

and $\mathbf{VI}(\Lambda, R_+^n)$ have precisely the same solutions, if any.

We are going to use the **Proposition 3.3** to prove the equivalence between the MMDUE and the VI problems formulated in Section 3.2.

3.3.1. Single-layer mode choice

Proof. From the UE conditions (5):

$$
\begin{aligned}
e^{-(\alpha^m + \beta_1 \mu_{m,t}^{rs})} &= \frac{h_{m,t}^{rs} \sum_{m'} e^{-(\alpha^{m'} + \beta_1 \mu_{m',t}^{rs})}}{q_t^{rs}} \\
\mu_{m,t}^{rs} &= \frac{1}{\beta_1} \left(-\left(\ln(h_{m,t}^{rs}) + \ln\left(\sum_{m'} e^{-(\alpha^{m'} + \beta_1 \mu_{m',t}^{rs})} \right) - \ln(q_t^{rs}) \right) - \alpha^m \right)
\end{aligned}
\tag{11}
$$

Then we have $c_{m,k,t}^{rs} - \mu_{m,t}^{rs} = c_{m,k,t}^{rs} + \frac{\alpha^m + \ln(h_{m,t}^{rs})}{\beta_1} + C(rs,t)$,where $C(rs,t) = \frac{1}{\beta_1} \ln\left(\frac{1}{q_t^{rs}} \sum_{m'} e^{-(\alpha^{m'} + \beta_1 \mu_{m',t}^{rs})} \right)$.

Suppose,

$$
\begin{aligned}
\Lambda_1 &= \{\Lambda_{k,t}^{rs}(\mathbf{f})\}, \quad \Lambda_{k,t}^{rs}(\mathbf{f}) = c_{m,k,t}^{rs}(\mathbf{f}) + \frac{\alpha^m + \ln h_{m,t}^{rs}}{\beta_1} \\
\tilde{\Lambda}_1 &= \{\tilde{\Lambda}_{k,t}^{rs}(\mathbf{f})\}, \quad \tilde{\Lambda}_{k,t}^{rs}(\mathbf{f}) = c_{m,k,t}^{rs}(\mathbf{f}) + \frac{\alpha^m + \ln h_{m,t}^{rs}}{\beta_1} + C(rs,t) \\
\forall \mathbf{f} &\in \Omega_1, \quad \Omega_1 = \{\mathbf{f} | \sum_k f_{m,k,t}^{rs} = q_t^{rs}\}
\end{aligned}
\tag{12}
$$

Let the vector $C = \{C(rs,t)\}$, since $C(rs,t)$ is identical for all paths of all modes between any fixed OD pair rs and departing time t, then $C^T(\mathbf{f} - \mathbf{f}^*)$ is 0, thus,

$$
\Lambda_1(\mathbf{f}^*)^T(\mathbf{f} - \mathbf{f}^*) = (\Lambda_1(\mathbf{f}^*) + C)^T(\mathbf{f} - \mathbf{f}^*) = \tilde{\Lambda}_1(\mathbf{f}^*)^T(\mathbf{f} - \mathbf{f}^*)
\tag{13}
$$

Therefore, $\mathbf{VI}(\Lambda_1, \Omega_1)$ is equivalent to $\mathbf{VI}(\tilde{\Lambda}_1, \Omega_1)$. Applying the DUE condition with equations above, we have $\tilde{\Lambda}_1(\mathbf{f}^*)^T \mathbf{f}^* = 0$. By **Proposition 3.3** we know the DUE is equivalent to $\mathbf{VI}(\tilde{\Lambda}_1, \Omega_1)$, hence it is also equivalent to $\mathbf{VI}(\Lambda_1, \Omega_1)$. $\qquad\square$

3.3.2. Two-layer mode choice

Proof. Similar to the proof of single-layer case in Section 3.3.1, from UE conditions (7) we have,

$$
\mu_{m,g(m),t}^{rs} = \frac{-\alpha_{g(m)}^m - \ln h_{m,g(m),t}^{rs}}{\beta_2^m} + \frac{\ln h_{m,t}^{rs}}{\beta_2^m} - \frac{\ln\left(\sum_{g' \in G(m)} e^{-(\alpha_{g'}^m + \beta_2^m \mu_{m,g',t}^{rs})} \right)}{\beta_2^m}
\tag{14}
$$

Also from UE conditions (7) we have $\mu_{m,t}^{rs} = -\frac{1}{\beta_2^m} \ln\left(\sum_{g' \in G(m)} e^{-(\alpha_{g'}^m + \beta_2^m \mu_{m,g',t}^{rs})} \right)$, then,

$$
c_{m,g(m),k,t}^{rs} - \mu_{m,g(m),t}^{rs} = c_{m,g(m),k,t}^{rs} + \frac{\alpha_{g(m)}^m + \ln h_{m,g(m),t}^{rs}}{\beta_2^m} - \frac{\ln h_{m,t}^{rs}}{\beta_2^m} - \mu_{m,t}^{rs}
\tag{15}
$$

From one-layer mode choice case, we have $\mu_{m,t}^{rs} = -\frac{\alpha^m + \ln(h_{m,t}^{rs})}{\beta_1} - C(rs,t)$, then,

$$
c_{m,g(m),k,t}^{rs} - \mu_{m,g(m),t}^{rs} = c_{m,g(m),k,t}^{rs} + \frac{\alpha_{g(m)}^m + \ln h_{m,g(m),t}^{rs}}{\beta_2^m} - \frac{\ln h_{m,t}^{rs}}{\beta_2^m} + \frac{\alpha^m + \ln(h_{m,t}^{rs})}{\beta_1} + C(rs,t)
\tag{16}
$$

Suppose,

$$
\begin{aligned}
\Lambda_2 &= \{\Lambda_{m,g(m),k,t}^{rs}(\mathbf{f})\}, \quad \Lambda_{m,g(m),k,t}^{rs}(\mathbf{f}) = c_{m,g(m),k,t}^{rs}(\mathbf{f}) + \frac{\alpha^m + \ln h_{m,t}^{rs}}{\beta_1} - \frac{\ln h_{m,t}^{rs}}{\beta_2^m} + \frac{\alpha_{g(m)}^m + \ln h_{m,g(m),t}^{rs}}{\beta_2^m} \\
\tilde{\Lambda}_2 &= \{\tilde{\Lambda}_{m,g(m),k,t}^{rs}(\mathbf{f})\}, \quad \tilde{\Lambda}_{m,g(m),k,t}^{rs}(\mathbf{f}) = c_{m,g(m),k,t}^{rs}(\mathbf{f}) + \frac{\alpha^m + \ln h_{m,t}^{rs}}{\beta_1} - \frac{\ln h_{m,t}^{rs}}{\beta_2^m} + \frac{\alpha_{g(m)}^m + \ln h_{m,g(m),t}^{rs}}{\beta_2^m} + C(rs,t) \\
\forall \mathbf{f} &\in \Omega_2, \quad \Omega_2 = \{\mathbf{f} | \sum_m \sum_{g(m)} \sum_k f_{m,g(m),k,t}^{rs} = q_t^{rs}\}
\end{aligned}
\tag{17}
$$

Similar to the proof of single-layer case in Section 3.3.1, since $C(rs,t)$ is identical for all paths of all modes between any fixed OD pair rs and departing time t, then $\mathbf{VI}(\Lambda_2, \Omega_2)$ is equivalent to $\mathbf{VI}(\tilde{\Lambda}_2, \Omega_2)$. Applying the DUE condition to the equations above, we have $\tilde{\Lambda}_2(\mathbf{f}^*)^T \mathbf{f}^* = 0$. By **Proposition 3.3** we know the DUE is equivalent to $\mathbf{VI}(\tilde{\Lambda}_2, \Omega_2)$, hence it is also equivalent to $\mathbf{VI}(\Lambda_2, \Omega_2)$. $\qquad\square$

3.4. Existence and uniqueness of the solution to MMDUE

We have proved the equivalence between MMDUE and its VI formulations in Section 3.3. So the existence and uniqueness of the solution to MMDUE is equivalent to the existence and uniqueness of the solution to the VI problems. In Nagurney (2009), the conditions for existence and uniqueness of solution to a general VI problem $\mathbf{VI}(\Lambda, \Omega)$ is provided and proved, see **Proposition 3.4**. It is proved using Brouwer's Fixed Point Theorem.

__Proposition 3.4__: If Ω is a compact convex set and $\Lambda(\mathbf{x}), \mathbf{x} \in \Omega$ is continuous on Ω, then the variational inequality problem $\mathbf{VI}(\Lambda, \Omega)$ admits at least one solution $\mathbf{x}^*$. If $\Lambda(\mathbf{x})$ is strictly monotone on Ω. Then the solution is unique, if one exists.

Given Ω_1, Ω_2 are both polyhedral, they are both compact convex sets. So the existence of solution depends on the continuity of $\Lambda_1(\mathbf{f}), \Lambda_2(\mathbf{f})$ on $\mathbf{f}$. From (6)(9) we know in Λ_1, Λ_2 all other terms apart from $c(\mathbf{f})$ are continuous with respect to $\mathbf{f}$. In $c(\mathbf{f})$, the only term associated with $\mathbf{f}$ is $w_{k,t}^{rs}$ based on the definition in (1-4), which is the actual travel time including car/bus/railway travel time, walking time, transfer time and parking cruising time calculated by the DNL model. In this research, we assumed the walking time is independent of path flow $\mathbf{f}$. Though the transfer time and the parking cruising time are dependent on $\mathbf{f}$ in our model, here we simplify them to be independent of $\mathbf{f}$ only to work with the solution existence. With this simplification, the existence of a solution solely depend on the continuity of car/bus/railway travel time on the path flow $\mathbf{f}$.

In the DNL process, railway travel time is almost constant according to the pre-determined railway schedule, car/bus travel time can be computed from different network traffic flow models. The continuity of exit-flow model was established by Wie et al. (1995) and point-queue model by Huang & Lam (2002), but for more complicated models like the cell transmission model (Daganzo 1995) and link queue model (Jin 2012), the continuity remains an open question. Under our MMDUE setting, the existence of the solution to the VI problem hence the MMDUE is extremely hard to prove rigorously, due to the complicated structure of our simulation model with cell-based traffic flow model, the possibility of link spill-back, and the different route choice behaviors and flow dynamics of multi-class vehicles. Since this is not the focus of this research, here we assume the VI problems $\mathbf{VI}(\Lambda_1, \Omega_1)$ and $\mathbf{VI}(\Lambda_2, \Omega_2)$ both admit at least one solution. However, the strict monotonicity of $\Lambda_1(\mathbf{f})$ on Ω_1 does not stand for general cases, according to **Proposition 3.4** the solution is not unique if one exists.

Even though the existence of the solution to MMDUE has not yet be proven rigorously, from a pragmatic standpoint, it is still necessary and advantageous to use this general framework of formulating and solving large-scale multi-modal network equilibrium with multi-class vehicles. Figure 4 is an abstraction of the MMDUE framework proposed in this paper at a higher level comparing to Figure 2. At the "Simulation" phase, the path travel costs are generated using multi-modal dynamic network loading, while at the "Updating" phase, the travelers' mode and route choices hence the network flow are updated using a gradient projection method that efficiently and effectively leads to convergence. We introduce the Simulation phase in Section 4 and the Updating phase in Section 5.
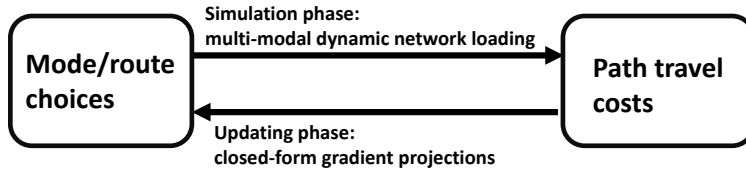

Figure 4: The high-level abstraction of the whole MMDUE framework.

Note for formulating and solving the MMDUE in a more applicable way, the OD demand for each time interval t is fixed, so there is no departure time choice in this paper. However, it is straightforward to extend MMDUE to accommodate departure time choice by relaxing the feasibility set Ω, e.g. relax Ω_1 to $\Omega_1 = \{\mathbf{f} | \sum_{k,t} f_{m,k,t}^{rs} = q^{rs} = \sum_t q_t^{rs}\}$. In the next section, a DNL model for computing the dynamic travel time $w_{k,t}^{rs}$ and hence $c_{m,k,t}^{rs}$ and $c_{m,g(m),k,t}^{rs}$ is introduced. Then the solution algorithm to the VI problems $\mathbf{VI}(\Lambda_1, \Omega_1), \mathbf{VI}(\Lambda_2, \Omega_2)$ is provided in Section 5.

4. Multi-modal Network Flow Simulation and Travel Time Estimation

The estimation of the travel time of each mode and path in the network is achieved by a mesoscopic DNL model. For example, as shown in Figure 5, the travel time of driving consists of car travel time from home to CBD

parking area, parking cruising time in the parking area and possibly a walking time from the parking area to the
destination. In the park-and-ride mode, the travel time consists of car travel time, parking cruising time, transfer
time (bus waiting time), bus travel time and walking time from the bus stop to the destination. For all travel modes,
the definitions of $w_{k,t}^{rs}$ in equation (1-4) are as follows:

$$
\begin{aligned}
\text{Driving:} \quad & w_{k,t}^{rs} = w_{k,t}^{rs}(\text{car travel}) + w_{k,t'}^{rs}(\text{parking cruising}) + w_{k,t''}^{rs}(\text{walking}) \\
\text{Ride-hailing:} \quad & w_{k,t}^{rs} = w_{k,t}^{rs}(\text{waiting}) + w_{k,t'}^{rs}(\text{car travel}) \\
\text{Transit:} \quad & w_{k,t}^{rs} = w_{k,t}^{rs}(\text{walking}) + w_{k,t'}^{rs}(\text{transfer/waiting}) + w_{k,t''}^{rs}(\text{bus/railway travel}) + w_{k,t'''}^{rs}(\text{walking}) \\
\text{Park-and-ride:} \quad & w_{k,t}^{rs} = w_{k,t}^{rs}(\text{car travel}) + w_{k,t'}^{rs}(\text{transfer/waiting}) + w_{k,t''}^{rs}(\text{bus/railway travel}) + w_{k,t'''}^{rs}(\text{walking})
\end{aligned}
\tag{18}
$$

Here $t < t' < t'' < t'''$ represents the start time of a trip component along a trip chain, such as "car travel",
"walking" or "bus travel", respectively. One component of a trip would start right after the end of the immediate
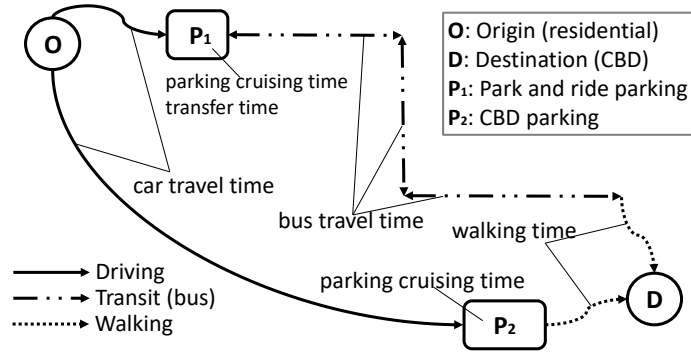past component.

Figure 5: An example of driving mode and park-and-ride mode: breakdown of the actual travel time.

4.1. Car/bus/railway travel time

The railway transit has its own infrastructure, and hence the railway travel time is assumed to be independent
of other modes. Its travel time follows the planned schedule and is not affected by the path flows $\mathbf{f}$ on the auto
network. However, most cars and buses share the same auto network to form mixed traffic. In this research,
the DNL model considers, on the auto network, heterogeneous vehicular flow propagation through links/nodes,
including light-duty vehicles and heavy-duty vehicles like buses and trucks. An example fundamental diagram of
class 1: passenger cars and class 2: buses and trucks are shown in Figure 6. Class 1 vehicles have larger free-flow
speed, maximum flow rate as well as jam density.

For modeling the heterogeneous vehicle flow on links, we adopted a multi-class traffic flow model proposed in
Qian et al. (2017), which can model the flow dynamics consisting of multiple classes of vehicles with distinct flow
characteristics. It pragmatically generalizes the cell transmission model (Daganzo 1994, Lebacque 1996) to multi-
class heterogeneous vehicle flow. It includes the concept "physical space split" for each class, which is the fraction
of physical space that each vehicle class occupies and uses to progress. Then the "perceived equivalent density"
of each class is calculated, representing the equivalent density perceived by some vehicle class, if converting
all other class vehicles to this class based on the space they occupied. At each loading time interval, vehicles
move through cells following the relations between upstream demand and downstream supply computed using
the "physical space split" and "perceived equivalent density", as well as the fundamental diagram of each class.
The main feature of this multi-class flow model is that it encapsulates three mixed flow regimes: one class can
overtake the other class under free flow, overtaking occurs restrictively under semi-congestion, and no overtaking
can occur under congestion. Details can be found in Qian et al. (2017) and Pi et al. (2019), comparing FASTLANE
by Van Lint et al. (2008).

Here we present a node model for vehicular flow evolution through junctions. For a junction j, we used a
relaxed version of the general node model introduced by Nie (2006). Denote the set of all upstream links by $A_{\rightarrow j}$,
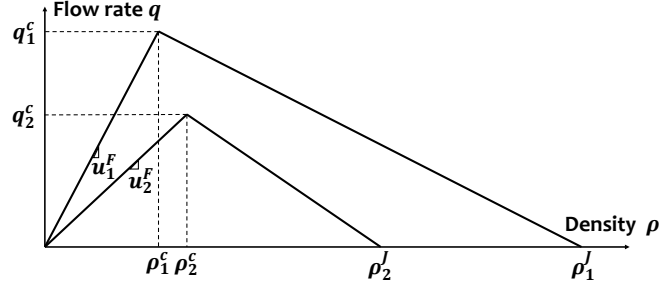
Figure 6: Fundamental diagrams of class 1: passenger cars and class 2: buses and trucks. u^F: free-flow speed, q^c: lane capacity, ρ^J: jam density.

and the set of all downstream links by $A_{j\rightarrow}$. Also denote the turning proportion from any upstream link $a \in A_{\rightarrow j}$ to any downstream link $b \in A_{j\rightarrow}$ at time t by $\psi_{a\rightarrow b}(t)$, where $\sum_{b\in A_{j\rightarrow}} \psi_{a\rightarrow b} = 1$, $\forall a \in A_{\rightarrow j}$. The flux from any upstream link $a \in A_{\rightarrow j}$ to downstream link $b \in A_{j\rightarrow}$ is $q_{a\rightarrow b}$:

$$q_{a\rightarrow b} = \min\left\{d_a(t)\psi_{a\rightarrow b}, s_b(t)\frac{d_a(t)\psi_{a\rightarrow b}}{\sum_{\alpha\in A_{\rightarrow j}} d_\alpha(t)\psi_{\alpha\rightarrow b}}\right\} \tag{19}$$

where, for any link a, the link demand $d_a(t)$ and supply $s_a(t)$ can also be computed for deciding the number of vehicles to be moved through the junctions.

Signalized junctions could also be applied to the network if data about signal timings are available. For large-scale mesoscopic simulation, the uncontrolled junction model (19) above usually works well enough for the estimation of travel states. It is also important to note that our model can successfully include the effect of queuing and spill-back in the dynamic network loading. The implementation of the above link and node models are shown in Figure 7, where the arrows represent how we move different classes of vehicles within the links and among different links through the nodes.
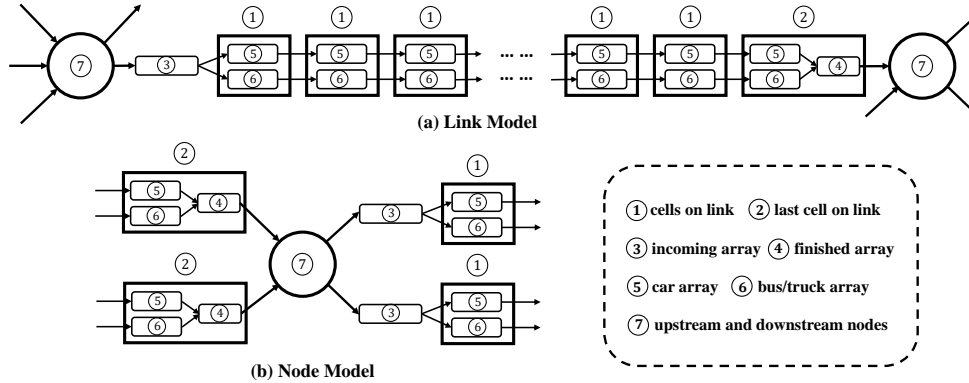

(a) Link Model

(b) Node Model

Figure 7: Implementation of link and node models.

As shown in Figure 7, the link model ensures first-in-first-out (FIFO) for each vehicle class separately, so the car and bus travel time can be computed using their respective cumulative curves. Cumulative curves are built by continuously counting and adding up the number of arriving and departing vehicles in each time interval. For each link i, there are one arrival and one departure curves for passenger cars $A_{1,i}(t)$ and $D_{1,i}(t)$, and similarly for buses/trucks $A_{2,i}(t)$ and $D_{2,i}(t)$. So the car and bus travel time departing at t from r to s along path k, if k consists of a link sequence $\{a_1, a_2, ..., a_n\}$, can be computed as follows:

$$
\begin{aligned}
w_{k,t}^{rs}(\text{car travel}) &= D_{1,a_n}^{-1}\left(A_{1,a_n}\left(D_{1,a_{n-1}}^{-1}\left(\cdots D_{1,a_1}^{-1}\left(A_{1,a_1}(t)\right)\right)\right)\right) - t \\
w_{k,t}^{rs}(\text{bus travel}) &= D_{2,a_n}^{-1}\left(A_{2,a_n}\left(D_{2,a_{n-1}}^{-1}\left(\cdots D_{2,a_1}^{-1}\left(A_{2,a_1}(t)\right)\right)\right)\right) - t
\end{aligned}
\tag{20}
$$

12

4.2. Parking cruising time

From day to day, parking cruising time is usually expected to depend on the expected parking occupancy in the targeted area. A typically expected parking space searching time function is approximately flat under low or medium occupancy but increases drastically when the occupancy is high and goes toward infinity when the parking area is full. Denote the parking occupancy of parking area i at time t by $e_i(t)$. If we assume all vehicles park in the parking area closest to their destinations, then $e_i(t)$ is determined by the network loading process, namely adding the number of vehicles arriving and subtracting the number of vehicles leaving. For studying the whole morning commute period, it is assumed at $t = 0$ the occupancy is zero, that is $e_i(0) = 0$ for all parking area i. A generic cruising time function is (Axhausen et al. 1994, Qian & Rajagopal 2014): $w_{k,t}^{rs}$(parking cruising) $= \mathbf{F}(e_i(t)) = \frac{\epsilon_i}{1-e_i(t)/E_i}$ where the parking area i is on path k, and the ϵ_i is the average parking time of a parking area when it is empty. E_i is the total capacity of the parking area. The parking occupancy $e_i(t)$ can be simulated through the multi-modal dynamic network loading process. It can also be estimated using historical parking data (Yang & Qian 2017) or predicted using real-time multi-source of traffic data using statistical and machine learning models (Yang et al. 2019).

In our numerical examples, the parking area represents an aggregation of both on-street/off-street parking spaces near the destination. Parking cruising time is included as part of the travel time in the generalized travel cost. The on-street cruising for parking and its impact to through traffic are currently not modeled in this specific DNL and numerical examples. However, the general MMDUE framework and solution algorithms proposed later still work for any generic dynamic simulation models. In the future, we plan to advance the study to explicitly model on-street parking cruising.

4.3. Travel time of other modes

The waiting time of bus/railway is simplified to a constant (e.g. historical average waiting time, or half of the headway), which is reasonable for high-frequency bus/railway service in morning commute peak hours (Pi et al. 2018, Zhang & Qian 2018). The historical average waiting time for the transit route at each transit stop is used in this study.

The walking time is proportional to the walking distance. Assuming the average walking speed is $\bar{v}$, then the walking time is $w_{k,t}^{rs}$(walking) $= l_{k,t}^{rs}/\bar{v}$, where $l_{k,t}^{rs}$ is the total walking distance in the route k at time t from r to s.

4.4. A comprehensive dynamic network loading (DNL) process

The DNL process runs for the whole study period (e.g. morning peak hours). The studying period was divided into 5-second discrete loading intervals. During each loading interval, the steps are performed as shown in **Algorithm [*NETWORK-LOADING*]**. After the whole loading process is completed, we can compute the time-dependent travel time for each link in the multi-modal network, and the generalized time/cost for paths along each OD. Mode split, link/path flow, and routes can also be updated. We discuss the detail of solution algorithms to MMDUE in the next section.

5. Solution to the MMDUE

To solve the MMDUE problems (5) and (7), we formulate them as VI problems $\mathbf{VI}(\Lambda_1, \Omega_1)$ in Equation 6 and $\mathbf{VI}(\Lambda_2, \Omega_2)$ in Equation 9, respectively. Solution algorithms to VI problems are categorized by: heuristic, projection-based and feasible direction algorithms. Heuristic algorithms often refer to the method of successive averages (MSA) (Sheffi 1985), which computes an all-or-nothing flow assignment based on time-dependent minimum-cost paths and then uses this flow assignment to update the old assignments as well as the costs of paths, repeat iteratively until converges. The projection-based algorithm obtains a new solution at each iteration i by solving $\mathbf{f}^{i+1} = \Pi_\Omega \left(\mathbf{f}^i - \tau \Lambda(\mathbf{f}^i) \right)$, where Π_Ω is the projection operator to the feasible set Ω of $\mathbf{f}$ (Han & Lo 2002, Lo & Szeto 2002). Feasible direction algorithms aims to find the strict ascent direction for the Generic merit function (GMF), $\theta(\mathbf{f}) = \min_{\mathbf{g}\in\Omega} \Lambda(\mathbf{f})^T(\mathbf{g} - \mathbf{f})$. Some example algorithms include Zhu & Marcotte (1993), Nie & Zhang (2010), Levin et al. (2015).

In this paper, we propose a new projection-based method for solving the VI problems, which has a closed-form representation for the path flow of each O-D pair. The new solution algorithm is more efficient than existing projection-based methods for large-scale networks.

Algorithm	**[*NETWORK-LOADING*]**
Step 0	*Initialization.* Initialize an empty network, as well as cumulative curves for each link.
Step 1	*Releasing.* For all origin nodes, generate different classes of vehicles, e.g. cars, trucks, buses, etc., according to vehicle demand and path flow. Release the vehicles to downstream links. For travelers choosing a transit mode, load them to the downstream transit network links.
Step 2	*Node evolution.* For all junction nodes in the auto network, move vehicles from upstream links to downstream links following Equation (19). Update the departure curves of upstream links and arrival curves of downstream links. For each parking nodes, store vehicles that enter and remove vehicles that exit the parking area, and update the parking occupancy. For transit stop nodes, load passengers on/off bus/train only if the bus/train arrives.
Step 3	*Link evolution.* For all auto network links, move vehicles on the links cell-by-cell following the multi-class traffic flow model (Qian et al. 2017). If a vehicle reaches the destination nodes, delete it from the network. For all bus network links, move the in-vehicle bus passengers as the propagation of buses on the auto network. For all railway network links, move the railway passengers according to the railway schedule.
Step 4	*Termination check.* Stop when the end of the study time period is reached. Otherwise, go to Step 1.

5.1. Closed-form gradient projection

The gradient projection methods solves the proposed VI formulation by minimizing the regularized merit function (RMF), presented by $\theta_\tau(\mathbf{f}) = \min_{\mathbf{g}\in\Omega} \Lambda(\mathbf{f})^T(\mathbf{g} - \mathbf{f}) + \frac{1}{2\tau}\|\mathbf{g} - \mathbf{f}\|_2^2$, where τ is a regularization weight and Ω can be either Ω_1 or Ω_2 in this study. One can prove that the optimal solution to $\theta_\tau(\mathbf{f})$ is the projection of $\mathbf{f} - \tau\Lambda(\mathbf{f})$ onto Ω (Facchinei & Pang 2007), as presented in $\mathbf{g}_\tau(\mathbf{f}) = \Pi_\Omega(\mathbf{f} - \tau\Lambda(\mathbf{f})) = \arg\min_{\mathbf{g}\in\Omega} \theta_\tau(\mathbf{f})$.

Also by Zhu & Marcotte (1993), $\mathbf{f} - \mathbf{g}_\tau(\mathbf{f})$ is a strict descent direction for either $\theta_\tau(\mathbf{f})$ at $\mathbf{f}$, or $\|\mathbf{g}_\tau - \mathbf{f}\|_2^2$ when $\Lambda(\mathbf{f})$ is Lipschitz continuous and monotone. Therefore, the proposed VI formulation can be solved by $\mathbf{f}^{i+1} = \mathbf{g}_\tau(\mathbf{f}^i)$ at each iteration i. Oftentimes, the projected gradient is solved by a quadratic programming solver, while in this paper we present a novel method that solves the projected gradient in a closed-form.

For each individual OD pair rs, we can expand the $\mathbf{g}_\tau(\mathbf{f})$ to a quadratic programming formulation presented in Equation 21.

$$\min_{\{g_{k,t}^{rs}\}_{k\in P_{rs}}} \sum_{k\in P_{rs}} \left(g_{k,t}^{rs} - f_{k,t}^{rs} + \tau\Lambda_{k,t}^{rs}\right)^2$$
$$\text{s.t.} \quad \sum_{k\in P_{rs}} g_{k,t}^{rs} = q_t^{rs} \tag{21}$$
$$g_{k,t}^{rs} \geq 0 \qquad \forall k \in P_{rs}, \ \forall t$$

where $P_{rs} = \cup_m P_m^{rs}$ for one-layer model and $P_{rs} = \cup_m \cup_{g(m)} P_{m,g(m)}^{rs}$ for the nested model. Note here all routes from all modes are indexed together and each route has a unique route indicator k. So, we omit the mode indicator m in the formulation above since the route indicator k implicitly include the mode choice. We can compute the gradients of $g_{k,t}^{rs}$ by solving Equation 21 in a quadratic solver. However, the dimension of $g_{k,t}^{rs}$ grows exponentially with the network size, and evaluating the gradients becomes highly time-consuming for large-scale networks. In this paper, we propose a new method to obtain the gradients by analyzing its Karush-Kuhn-Tucker (KKT) conditions.

The KKT conditions of the formulation (Equation 21) are as follows:

$$
\begin{array}{lll}
\text{Stationarity:} & -2 \ (g_{k,t}^{rs} - f_{k,t}^{rs} + \tau\Lambda_{k,t}^{rs}) = \lambda - \mu_{k,t}^{rs} \\
\text{Primal feasibility:} & g_{k,t}^{rs} \geq 0, \ \sum_{k\in P_{rs}} g_{k,t}^{rs} = q_t^{rs} \\
\text{Dual feasibility:} & \mu_{k,t}^{rs} \geq 0 \\
\text{Complementary slackness:} & \mu_{k,t}^{rs} \ g_{k,t}^{rs} = 0, \forall k
\end{array} \tag{22}
$$

where $\mu_{k,t}^{rs}$ and λ are the dual variables. Combining the four conditions, if $\mu_{k,t}^{rs} = 0$, $g_{k,t}^{rs} = f_{k,t}^{rs} - \tau\Lambda_{k,t}^{rs} - \frac{\lambda}{2}$, and if $\mu_{k,t}^{rs} > 0$, $g_{k,t}^{rs} = 0$. Also, by Primal feasibility we have $\sum_{k\in P_{rs}} g_{k,t}^{rs} = q_t^{rs}$. Then $\frac{\lambda}{2} = -\frac{\tau}{|P_{rs}|} \sum_{k\in P_{rs}} \Lambda_{k,t}^{rs}$. So for each

iteration we choose $0 < \tau \leq \frac{1}{\max_k \left(c_{k,t}^{rs} - \frac{1}{|P_{rs}|} \sum_{k' \in P_{rs}} c_{k',t}^{rs} \right)}$, the solution to the problem formulation (21) is presented by:

$$g_{k,t}^{rs} = f_{k,t}^{rs} - \tau \left(c_{k,t}^{rs} - \frac{1}{|P_{rs}|} \sum_{k' \in P_{rs}} c_{k',t}^{rs} \right) \tag{23}$$

The difference between the quadratic solver and our method is that our method has an analytical form if we decompose the whole problem into individual OD pair. By analyzing the KKT conditions, we can get the gradients of the decision variables without solving any optimization problem. The trick we are using is to adaptively choose τ in each iteration to satisfy the condition $0 < \tau \leq \frac{1}{\max_k \left(c_{k,t}^{rs} - \frac{1}{|P_{rs}|} \sum_{k' \in P_{rs}} c_{k',t}^{rs} \right)}$. In this paper, we choose $\tau = \frac{1}{\max_k \left(c_{k,t}^{rs} - \frac{1}{|P_{rs}|} \sum_{k' \in P_{rs}} c_{k',t}^{rs} \right)}$ for each iteration. More importantly, existing quadratic solver has to work with the path flow of all OD pairs simultaneously which is computationally heavy, whereas our method computes the solutions for the flow of each OD pair separately. Clearly, our method can adapt to very large-scale networks. Therefore, one can expect that our method is more efficient in large-scale networks. In the experiments, we also observe that our method achieves a better convergence rate than the original quadratic solver method.

Note here the $c_{k,t}^{r,s}$ is exactly the generalized path travel cost $c_{m,k,t}^{r,s}$ we defined in section 3, with the mode indicator m omitted since the route indicator k implicitly include the mode choice. It is calculated and updated from the multi-modal dynamic network loading process in every iteration of our MMDUE algorithm, see section 5.2.

5.2. Solution framework

The proposed formulation is path based. The number of paths with positive flow increases exponentially when the network and number of modes grows. We adopt the column generation method to augment the path set at each iteration (Nie & Zhang 2007), and the time-dependent shortest path (TDSP) algorithm (Chabini 1998) is run on the combined multi-modal graph to search for the shortest path across different modes. The solution framework of the MMDUE problem (5)(7) is summarized in **Algorithm [*MMDUE-SOLVER*]**.

Algorithm	**[*MMDUE-SOLVER*]**
Step 0	*Initialization.* Initialize a path set, and initialize the path flow vector **f** such that the passenger demand **q** is evenly distributed to each path.
Step 1	*Dynamic network loading.* Generate vehicular demand from the passenger flow. Run a full [*NETWORK-LOADING*] process (section 4.4) with vehicular flow, and obtain the generalized path cost for each path.
Step 2	*Passenger path set augmentation.* Run a time-dependent shortest path algorithm on the graph presented in Figure 1 with the travel costs obtained in *Step 1*, and append the shortest path to the path set P^{rs}.
Step 3	*Update passenger flow.* Update the passenger path flow with the travel costs obtained in *Step 1* using the gradient projection method presented in section 5.1.
Step 4	*Convergence check.* Stop when the path set P^{rs} does not change and the change of path flow **f** is less than tolerance. Otherwise, go to Step 1.

6. Numerical Experiments

We first solve the MMDUE in a simplified multi-modal network in Pittsburgh. The effectiveness and efficiency of the proposed gradient projection method are examined. The sensitivity analysis with respect to parameters is thoroughly explored for policy insights. To show the convergence performance and the efficiency of our model and algorithms on large-scale networks, we also test it on a large-scale multi-modal network of the SR-41 network in Fresno, California.

6.1. A simplified multi-modal network for downtown and southern Pittsburgh

The MMDUE model is tested in the network shown in Figure 8. The network is an abstraction of the real multi-modal network in the Pittsburgh region, covering the district of Upper St Clair, Bridgeville, Mt Lebanon, Scott Township, Carnegie, Green Tree, Banksville, Mt Washington and Downtown Pittsburgh, with I-79, I-376, US Route 19 and a light rail Red Line connecting the suburbs and the downtown, see Figure 8(b). The simplified network is shown in 8(a), with five origins $O_1 \sim O_5$, one destination D_1, nine nodes (junctions), 16 links (road segments), three parking areas, one bus route, and one railway line. The parking area can be viewed as the aggregation of all parking space in that area, and we only considered one bus route that represents the aggregation of all high-frequency routes and one railway line. We also assume all travelers own or have access to a private car, which means $\xi = 0$. This allows all travelers to choose any travel modes in this experiment.
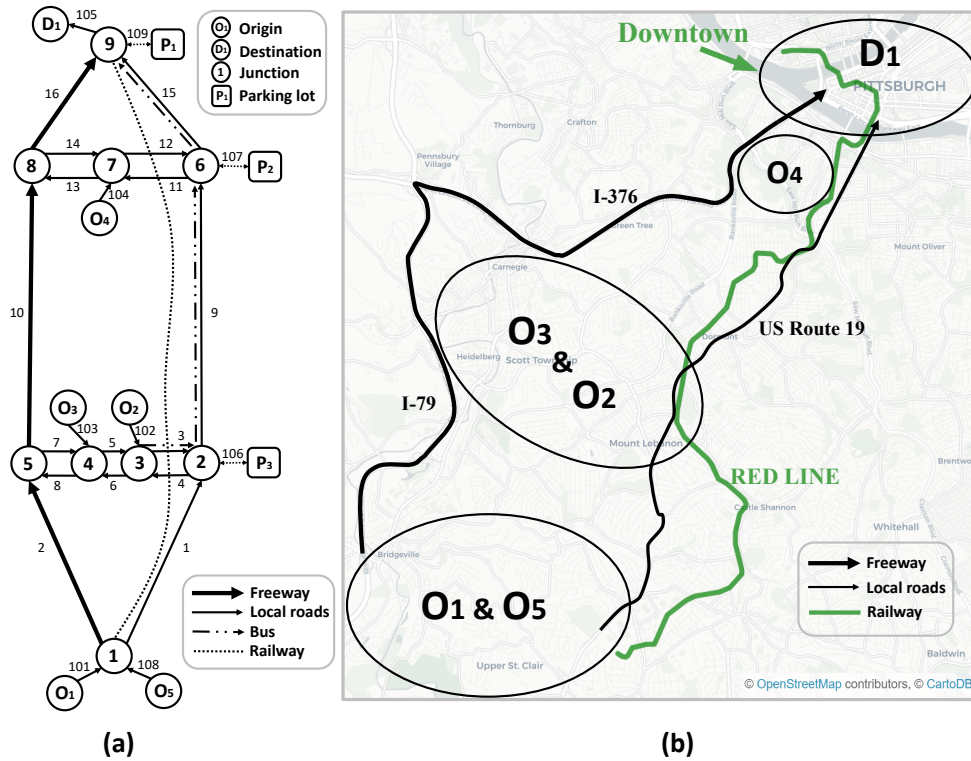

Figure 8: (a) A simplified multi-modal network for downtown and southern Pittsburgh region used in the experiments. Note the bus line represents the aggregation of all high-frequency bus routes in this area. Nodes and links are labeled on the figure. (b) The real network map. Origins 1 to 5 are all large residential zones. Downtown (D1) is the only destination.

We have made efforts on calibrating the traffic flows and OD demand in the Pittsburgh metropolitan area in a separate project (Ma & Qian 2015, Ma et al. 2019, Ma & Qian 2018), so the OD demands were employed in this study. The total passenger demand is set as 30,000 for the morning peak hours (5 AM to 9 AM) in this area, from all origins $O_1 \sim O_5$ to the only destination D_1. Note origins $O_1 \sim O_5$ are all large residential districts, and the only destination D_1 is downtown Pittsburgh. All link parameters are listed in Table 1 and all modes and paths are listed in Table 2. O_2 is the bus origin and only for releasing buses to the network. O_5 is the truck origin and only for releasing trucks to the network. All other parameters used in the experiment are listed in Table 3.

6.1.1. Convergence

We solve the MMDUE with the solution framework presented in section 5.2. Changes in the equilibrium gap against the number of iterations using our proposed solution and quadratic solver are presented in Figure 9. All the experiments below are conducted on a desktop with Intel Core i7-6700K CPU @ 4.00GHz × 8, 2133 MHz 2 × 16GB RAM, 500GB SSD. We run our algorithm for 100 iterations, and the proposed method outperforms the

Table 1: Link parameters. u^F: free-flow speed, q^c: lane capacity, ρ^J: jam density. Subscript 1: passenger cars, 2: buses and trucks.

Link	Length (mile)	# of lanes	u_1^F (mph)	u_2^F (mph)	q_1^c (veh/hour)	q_2^c (veh/hour)	ρ_1^J (veh/mile)	ρ_2^J (veh/mile)
l_1 ($n_1 \to n_2$)	4.00	2	40	35	2000	1200	200	100
l_2 ($n_1 \to n_5$)	4.50	3	65	55	2300	1200	200	100
l_3 ($n_3 \to n_2$)	1.50	1	30	25	1800	1000	200	100
l_4 ($n_2 \to n_3$)	1.50	1	30	25	1800	1000	200	100
l_5 ($n_4 \to n_3$)	0.55	1	30	25	1800	1000	200	100
l_6 ($n_3 \to n_4$)	0.55	1	30	25	1800	1000	200	100
l_7 ($n_5 \to n_4$)	2.50	1	30	25	1800	1000	200	100
l_8 ($n_4 \to n_5$)	2.50	1	30	25	1800	1000	200	100
l_9 ($n_2 \to n_6$)	4.50	2	40	35	2000	1200	200	100
l_{10} ($n_5 \to n_8$)	6.00	3	65	55	2300	1200	200	100
l_{11} ($n_6 \to n_7$)	0.50	1	30	25	1800	1000	200	100
l_{12} ($n_7 \to n_6$)	0.50	1	30	25	1800	1000	200	100
l_{13} ($n_7 \to n_8$)	0.50	1	30	25	1800	1000	200	100
l_{14} ($n_8 \to n_7$)	0.50	1	30	25	1800	1000	200	100
l_{15} ($n_6 \to n_9$)	1.50	2	40	35	2000	1200	200	100
l_{16} ($n_8 \to n_9$)	1.50	3	65	55	2300	1200	200	100

Table 2: All modes and paths in the numerical experiment.

Path name	Origin	Destination	Mode	Sub-mode	Path
Path 1	O_1	D_1	driving	solo	$l_{101} \to l_2 \to l_{10} \to l_{16} \to l_{105}$
Path 2	O_1	D_1	driving	solo	$l_{101} \to l_1 \to l_9 \to l_{15} \to l_{105}$
Path 3	O_1	D_1	driving	carpool	$l_{101} \to l_2 \to l_{10} \to l_{16} \to l_{105}$
Path 4	O_1	D_1	transit	railway	$l_{101} \to$ railway line $\to l_{105}$
Path 5	O_1	D_1	park&ride	driving+bus	$l_{101} \to l_1 \to l_{106} \to P_3 \to l_{106} \to l_9 \to l_{15} \to l_{105}$
Path 6	O_1	D_1	park&ride	driving+bus	$l_{101} \to l_2 \to l_7 \to l_5 \to l_3 \to l_{106} \to P_3 \to l_{106} \to l_9 \to l_{15} \to l_{105}$
Path 7	O_1	D_1	park&ride	driving+bus	$l_{101} \to l_1 \to l_9 \to l_{107} \to P_2 \to l_{107} \to l_{15} \to l_{105}$
Path 8	O_1	D_1	park&ride	driving+bus	$l_{101} \to l_2 \to l_{10} \to l_{14} \to l_{12} \to l_{107} \to P_2 \to l_{107} \to l_{15} \to l_{105}$
Path 9	O_3	D_1	driving	solo	$l_{103} \to l_8 \to l_{10} \to l_{16} \to l_{105}$
Path 10	O_3	D_1	driving	solo	$l_{103} \to l_5 \to l_3 \to l_9 \to l_{15} \to l_{105}$
Path 11	O_3	D_1	driving	carpool	$l_{103} \to l_8 \to l_{10} \to l_{16} \to l_{105}$
Path 12	O_3	D_1	transit	bus	$l_{103} \to l_5 \to l_3 \to l_9 \to l_{15} \to l_{105}$
Path 13	O_3	D_1	park&ride	driving+bus	$l_{103} \to l_5 \to l_3 \to l_{106} \to P_3 \to l_{106} \to l_9 \to l_{15} \to l_{105}$
Path 14	O_4	D_1	driving	solo	$l_{104} \to l_{13} \to l_{16} \to l_{105}$
Path 15	O_4	D_1	driving	solo	$l_{104} \to l_{12} \to l_{15} \to l_{105}$
Path 16	O_4	D_1	driving	carpool	$l_{104} \to l_{13} \to l_{16} \to l_{105}$
Path 17	O_4	D_1	park&ride	driving+bus	$l_{104} \to l_{12} \to l_{107} \to P_2 \to l_{107} \to l_{15} \to l_{105}$
Bus route	O_2	D_1	N/A	N/A	$l_{102} \to l_3 \to l_9 \to l_{15} \to l_{105}$
Through truck traffic	O_5	D_1	N/A	N/A	$l_{108} \to l_2 \to l_{10} \to l_{16} \to l_{105}$

Table 3: All other model parameters.

Name	Values				
Morning commute model	$\alpha = \$6.4$/hour	$\beta = \$3.9$/hour	$\gamma = \$15.2$/hour	$t^* = 9$AM	
Logit model	$\alpha^1, \alpha^1_{g(1)\in G(1)} = 1.5$	$\alpha^2, \alpha^2_{g(2)\in G(2)} = 1.0$	$\alpha^4, \alpha^4_{g(4)\in G(4)} = 2.0$	$\beta_1 = 1.0$	$\beta_2^{m\in\{1,2,4\}} = 1.0$
Parking-1 (CBD)	$p_1 = \$10$	$\epsilon_1 = 2$ min	$E_1 = 10000$		
Parking-2	$p_2 = \$3$	$\epsilon_2 = 1$ min	$E_2 = 20000$		
Parking-3	$p_3 = \$3$	$\epsilon_3 = 1$ min	$E_3 = 20000$		
Bus	$\delta_k^{rs} = \$2.75$	$\sigma_{k,t}^{rs} = 0$	frequency = 15 min	waiting = 7.5 min	
Railway	$\delta_k^{rs} = \$3.75$	$\sigma_{k,t}^{rs} = 0$	frequency = 12 min	waiting = 6.0 min	full trip = 40.0 min
Carpooling	$\Delta_{k,t}^{rs}(1) = 0$	$\Delta_{k,t}^{rs}(2) = \$1$			
Dynamic network loading	unit time = $5s$	# of intervals = 2880	start time = 5AM	end time = 9AM	

quadratic optimization method in terms of the equilibrium gap. It takes the proposed method 211s to complete 100 iterations, comparing to the 227s taken by the quadratic solver.
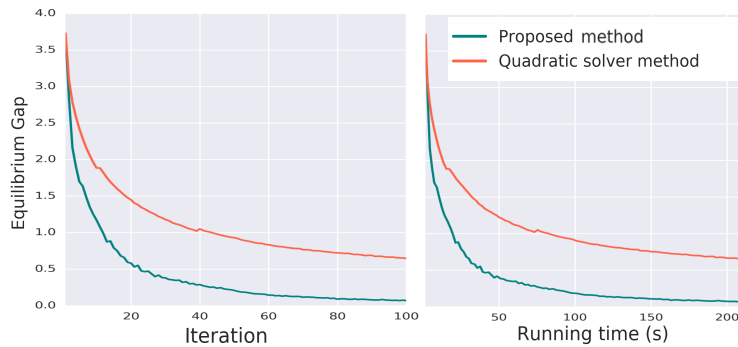

Figure 9: Convergence curves for both gradient projection methods.

6.1.2. Solution of network flow and mode choices

The path choice probability over the morning peak for OD pair $(1, 1)$ and OD pair $(3, 1)$ is presented in Figure 10. For OD pair $(1, 1)$, most travelers departing in 5 AM-6 AM choose carpool and railway to commute, and more travelers select park-and-ride (PnR) after 7 AM. The generalized cost of metro is relatively low, as a result of low railway fare. After 8 AM, taking railway will incur a high late arrival cost penalty, so the path flow of railway decreases dramatically. Using carpool directly to CBD is another preferred choice before 8 AM since the roads to CBD are not congested yet. After 8 AM, cruising time for parking in the CBD area increases, leading to a decline in the carpool probability. In contrast, the generalized park-and-ride cost is low when the CBD is congested because of the savings on travel time and parking fee. Hence park-and-ride mode becomes the most preferable choice after 8 AM. At 7 AM, the flow of paths 7 and 8 has a spike, possibly due to the unstable UE solution when the cost of path 7 and 8 coincide. The stability of MMDUE can be improved in future research by the method proposed by (Tobin & Friesz 1988, Patriksson 2004). Similar choice patterns can be observed for OD pair $(3, 1)$. One observation is that there are few travelers choosing solo-driving all the way to downtown, which is probably attributed to the high parking fee in the downtown, relatively low inconvenience cost for carpool, and the way transit and park-and-ride are provided in this experiment.
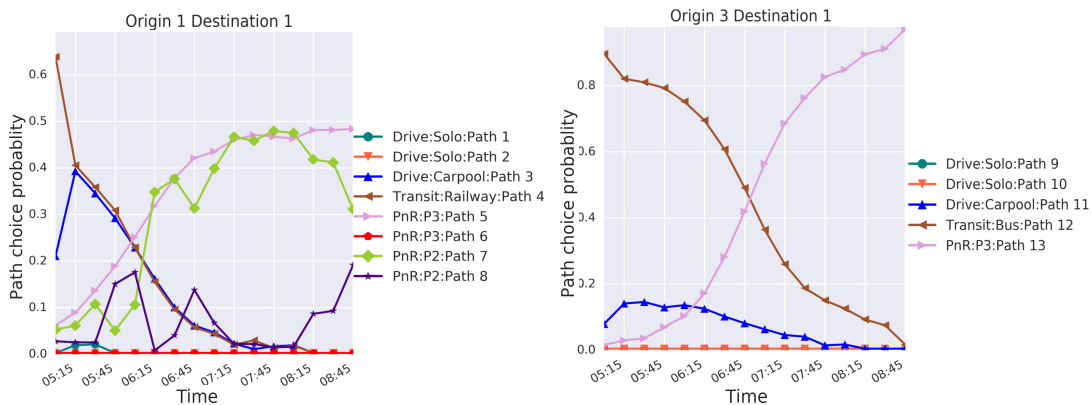

Figure 10: Time-varying path choice for OD pair $(1, 1)$ and $(3, 1)$.

6.1.3. Sensitivity analysis on total demand level

We change the total demand from 75% to 125% of the O-D demand in the original problem settings, keeping other parameters the same. We solve the MMDUE under different demand levels and plot the average user cost for different modes and the route choice for OD pair (1,1) in Figure 11.
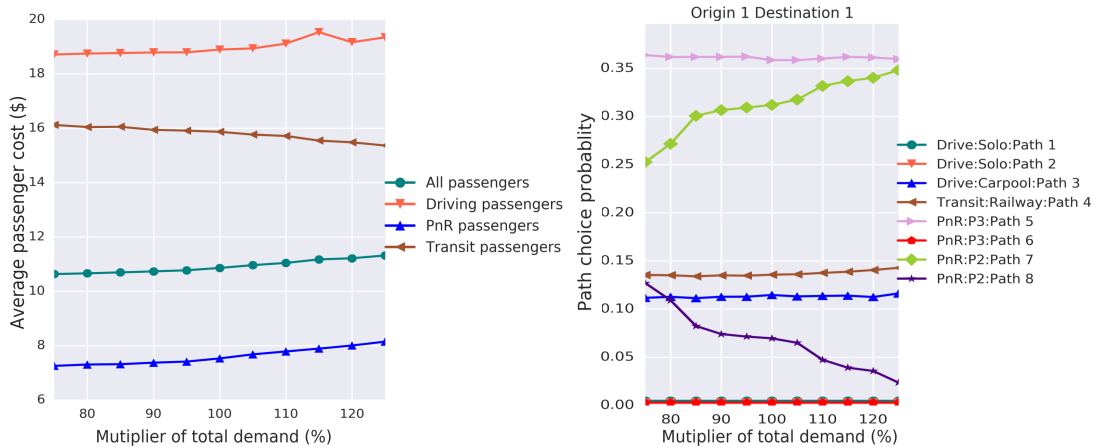
Figure 11: The influence of total demand on average cost per traveler and the path choice for OD pair (1,1).

It shows clearly the average passenger cost increases with respect to the demand level, and the influence of demand level to the average cost is approximately "linear". The cost of driving passengers and park-and-ride passengers increase since the network become over-saturated, while the cost of transit passengers almost remain the same, as a result of constant railway cost. Also, the increasing demand will generally force travelers to avoid driving in routes with high congestion levels. Hence for OD $(1, 1)$, the park-and-ride flow drops on Path 8 and increases on Path 7, as a result of more and more congested highways/freeways. Figure 11 can be used to determine the marginal travel time/cost at different demand levels, which supports the urban planning for policymakers.

6.1.4. Sensitivity analysis on parking and bus fare

We study the joint influence of bus fare and parking fare. We change the bus fare and parking fare by applying a multiplier to the fare in the original settings, which ranges from 1 to 5. We solve the MMDUE under different bus and parking fares, and plot the average cost for all travelers, driving travelers, transit travelers and park-and-ride travelers in Figure 12.

When the bus fare increases, the average traffic cost and average park-and-ride cost increase. This is because the park-and-ride cost includes bus fare and park-and-ride is one of the most preferred modes for all travelers. When the parking fare increases, the average costs of driving and park-and-ride increase substantially, because in both modes the travelers need to pay for the parking fee. In this case, the average traffic cost also increases. One interesting observation is that the average transit cost is relatively stable, which implies that transit cost has little change when bus fare and parking fare is changing. One important reason is that transit passengers do not pay the parking fare, and another reason is that many transit passengers can switch from bus to railway. Travel cost incurred on the railway model does not change as much regardless of parking or bus fare.

6.1.5. Influence of inconvenience (impedance) cost

In the original settings, the inconvenience (impedance) costs for carpool, transit, and park-and-ride are assumed to be at a very low level for testing the MMDUE model and the algorithm. As a result, the driving flow is marginal in the MMDUE solutions, which is deviated from the real situation in the study area. In this section, we will explore the impact of inconvenience cost on travelers' mode choice. We set the inconvenience costs for carpool, transit, and park-and-ride to be \$5 under MMDUE. The path choice probability over the morning peak for OD pairs $(3, 1)$ and $(4, 1)$ is presented in Figure 13. Generally, more travelers in O_3 and O_4 choose solo-driving before 7 AM, due to higher (inconvenience) costs for transit/park-and-ride. To conclude, the inconvenience costs has a considerable impact on travelers' mode choice. Therefore, public transit with great accessibility effectively attracts travelers. In future studies, a more fine-grained model should be developed to estimate the values of inconvenience costs, for example, there should be different inconvenience costs for groups of travelers with different demographic or traveling characteristics.
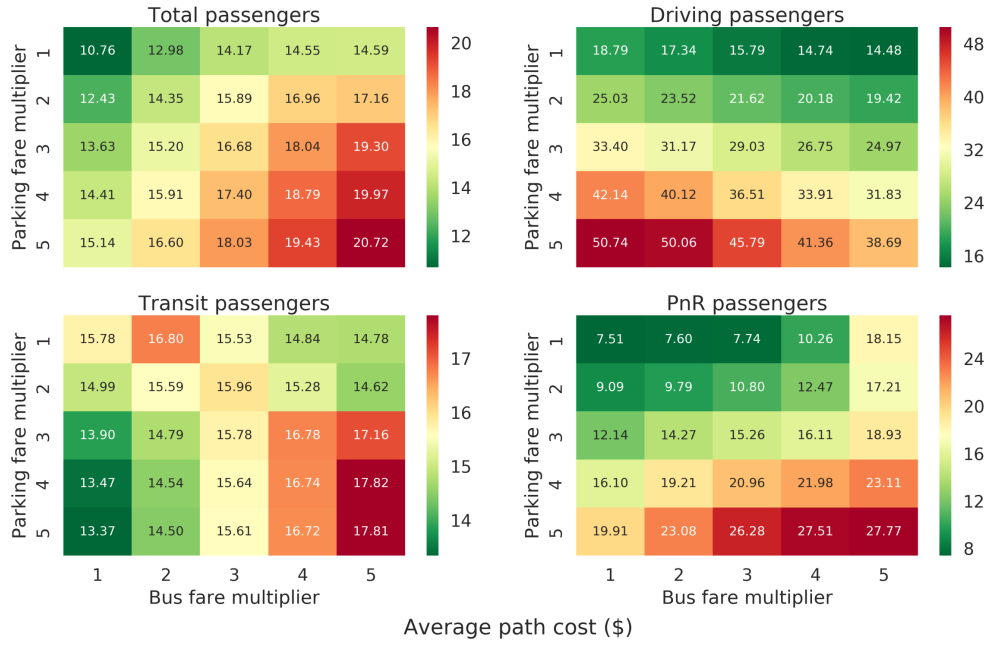
Figure 12: Heatmap of average cost for total traffic and different modes.

6.2. A large-scale multi-modal network for SR-41, California

To show the convergence performance and the efficiency of our model and algorithms on large-scale networks, we also test our model and algorithms on a large-scale multi-modal network for SR-41, California. It is located at Fresno, California, with SR-41 highway in the center, see Figure 14. It contains 2,065 links, 1,441 nodes and 7,110 OD pairs. The public transit system is operated by the Fresno Area Express (FAX). There are 16 bus routes operated in this network, including route 1 southbound, route 9 eastbound/westbound, route 28 eastbound/westbound, route 32 southbound, route 33 eastbound/westbound, route 34 southbound/northbound, route 35 eastbound/westbound, route 39 eastbound/westbound, and route 41 eastbound/westbound. There is no railway traffic in this network. There are also 199 parking lots scattered in this network, near important intersections or other locations in the city. The travel demand for this network is in all 170,399 for the 3-hour morning peak period, obtained from previous research Liu et al. (2006) and Zhang, Ma, Singh & Chu (2008). We also assume all travelers own or have access
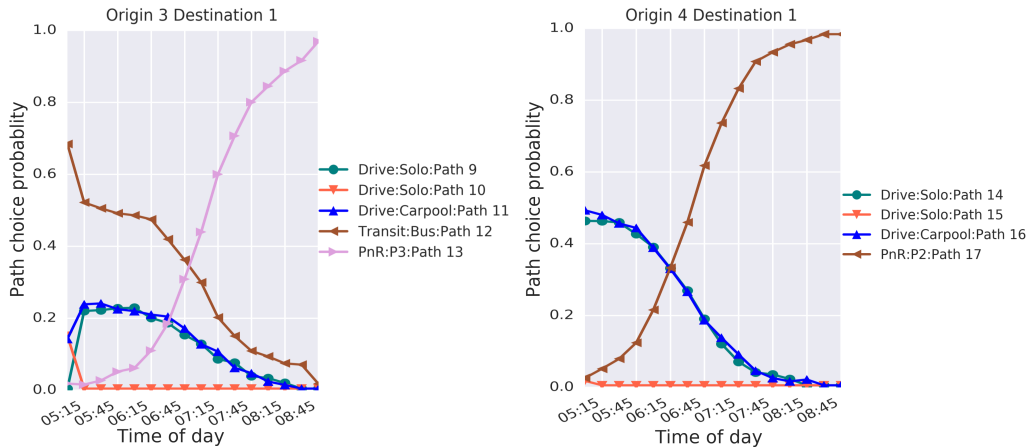

Figure 13: Time-varying path choice for OD pairs (3,1) and (4, 1) with high inconvenience costs.

20

to a private car, which allows all travelers to choose any of the three travel modes including driving, park-and-ride and bus transit. The parameters in the morning commute model and nested logit model are used the same as shown in Table 3.
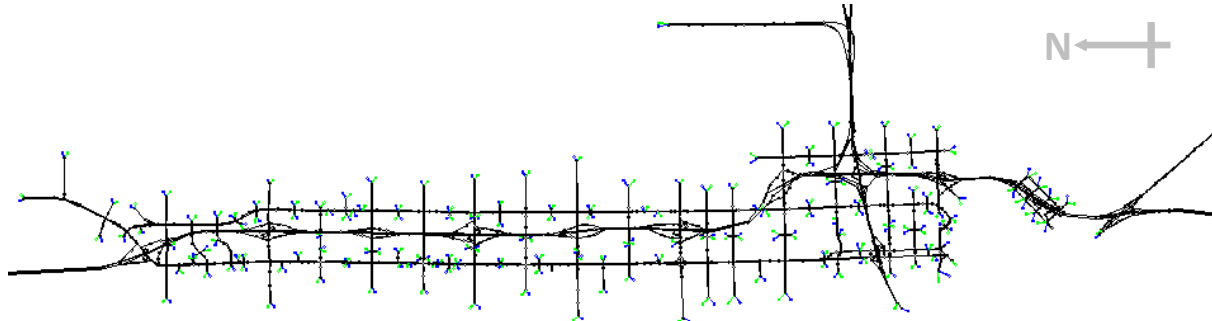

Figure 14: The SR41 network.

For multi-modal large-scale networks, how to generate the feasible path set for each OD pair with several travel modes is challenging. In this study, the path set is generated for each travel mode separately. For driving, three shortest paths are computed on the auto network, each under one of the three traffic conditions: free-flow, mild congestion and severe congestion. For bus transit, the paths are generated by finding the feasible bus routes connecting the origin and destination with a total walking distance less than a threshold, namely 500m. Finally, the paths for park-and-ride are also generated by finding the shortest paths on the combined multi-modal network, with the total walking distance being limited to be less than the threshold. Limiting the walking distance among parking, bus stops and origins/destinations allows efficient searching for feasible paths. In this study, we generate in all 8,813 paths for solo-driving and carpool travelers, 344 paths for bus transit, and 1,205 paths for park-and-ride travelers. We use the pre-determined fixed path sets for each mode. The path set could also be generated from the combined multi-modal network in a dynamic fashion using a column generation method, which is more computationally intensive but may help improve the equilibrium results. We are also going to explore the influence of fixed/dynamic path set on the equilibrium results in our future study.
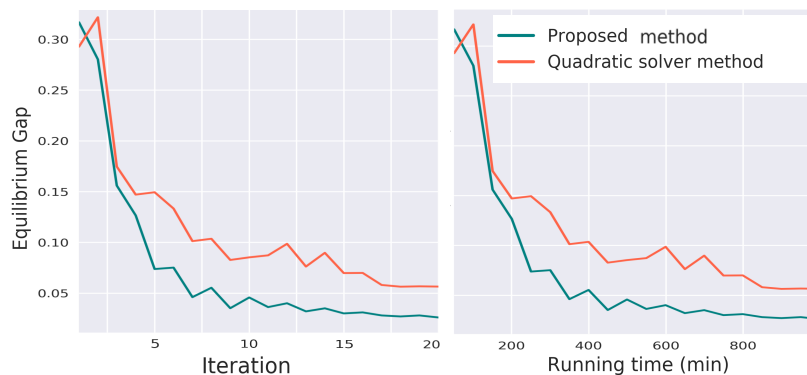

Figure 15: The convergence performance for both gradient projection methods in the SR41 network.

The convergence of both our proposed gradient projection method and the quadratic solver is presented in Figure 15. The results show our proposed method considerably outperforms the quadratic solver in both equilibrium gap and computational time. In large-scale experiments, the dynamic network loading process and the calculation of generalized cost for each path are computationally intensive in addition to the gradient projection. Thus, the overall computational efficiency could be improved significantly if we can speed up those two components in the future. In conclusion, this experiment shows the applicability and efficiency of applying our model and solution algorithms to large-scale networks that consist of thousands of links, nodes, and OD pairs, as well as a large feasible path set.

7. Conclusion

This paper formulates and solves a general dynamic traffic assignment problem for multi-modal dynamic networks. It estimates spatio-temporal passenger and vehicular flows in a general multi-modal network that explicitly considers parking and many conventional and emerging travel modes, including solo-driving, carpooling, ride-hailing, bus transit, railway transit, and park-and-ride. Vehicular flows, namely cars, trucks, and buses, as well as passenger flow, are integrated into a holistic dynamic network loading (DNL) models with heterogeneous traffic flow, transit, parking, and mode transfer. Travel behavior of passenger demand on modes choice is encapsulated by a multi-layer nested logit model. We formulate a general multi-modal dynamic user equilibrium (MMDUE) as a Variational Inequality (VI) problem. A new gradient projection method is proposed and shown to efficiently solve the VI problem on large-scale networks.

Numerical experiments are conducted on a multi-modal network of the Pittsburgh region along with sensitivity analysis with respect to demand, infrastructure features, and management strategies. We show that total passenger demand, parking prices, transit fare and ride-sharing impedance can effectively impact both system performance and individual user costs. This indicates transportation system planning and operation require a holistic solution across all modes. Experiments on a large-scale multi-modal network in Fresno, California also show our model and solution method has good convergence performance and computational efficiency. The proposed theory and algorithms provide a possible comprehensive solution for managing such complex multi-modal transportation networks.

The general framework of the MMDUE formulation and solution proposed in this paper is a complete inclusion of most travel modes existed in modern urban traffic systems. However, except for few metropolitans, most cities or towns do not have all travel modes discussed in this paper. Our MMDUE framework, in these cases, could be reduced to simpler cases, for example, bi-modal choices, driving with parking choices, etc. The MMDUE framework is flexible enough for being applied to different scenarios and hence to be useful in most urban traffic systems. We introduce some example scenarios as follows: (1) Solo-driving and carpooling: For small cities or towns without public transit and ride-hailing service, solo-driving and carpooling are almost the only travel modes for daily commuting if we don't consider walking for long distance. In this case, the general framework is reduced to two-mode choices, solo-driving and carpooling. Travelers choose solo-driving and carpooling based on the travel time and carpooling impedance. The network in our MMDUE framework now only consists of the auto network, so the routing is performed on the auto network and path sets should be relatively smaller than similar scale multi-modal networks with extra virtual bus network and railway network. The DNL model could also be simplified to homogeneous traffic since only passenger car flow and travel time are required. (2) Driving with parking choices: If parking behavior is also considered, then different parking areas should be added to the network. In this case, travelers choose solo-driving or carpooling, as well as choosing the parking location with the lowest total travel cost. The parking costs including the parking cruising time and parking fee will both affect the traveler's choice heavily, unveiled by previous studies (Qian et al. 2012, Qian & Rajagopal 2014). Long parking cruising time and high parking fee can enforce traveler to park farther and walk to their final destination. A high parking fee will also encourage carpooling since carpoolers can share the parking fee together. The DNL in this case should explicitly model the parking area occupancy at each time interval for estimation of the dynamic parking cruising time. The MMDUE solution will show not only the dynamic states of the auto network but also the dynamic evolution of parking occupancy of each parking area. (3) Driving and transit: For cities with the public transit system, if parking and park-and-ride are not considered, then travelers choose travel modes from driving, bus transit and possibly railway transit. The feasible path set for each OD should include all feasible paths under each mode. So the path set generation and routing are always performed on the auto network, virtual bus network and railway network all combined as shown in Figure 1. DNL model should run with multi-class vehicles on the auto network, and different link travel time of passenger cars and buses should be computed. Based on the MMDUE framework, the influence of new public transit routes, new stops, and other developing mass-transport classes like demand responsive transit and microtransit can be studied (Xu et al. 2016, 2017). The MMDUE framework can also be used to evaluate and optimize the public transit schedules, trip frequencies, bus/train size and seat numbers and other operational strategies.

The proposed MMDUE model serves as an underlying model to support holistic decision making for planning and traffic management, at any spatial scale. What is not addressed in this paper is how to calibrate the parameters of MMDUE to best fit the real-world data acquired from conventional and emerging sensors in the multi-modal

network. The process of model calibrating with day-to-day multi-modal data will be our research focus in the near future. Also, the outcome of this paper serves as a general framework of large-scale multi-modal network modeling and equilibrium analysis with the inclusion of many different travel modes, some of which are simplified like the ride-hailing mode. In our future research, we are going to extend and apply this framework to different scenarios, especially the cases with shared travel modes, for example, the networks with driving and ride-hailing (Xu et al. 2019*b*, Xu et al. 2019*a*), or ride-hailing and public transit, etc. Another extension to this study is to incorporate the uncertainties, for example, uncertainties from traveler's cost function, uncertainties from travel demand (Pi & Qian 2017), etc. which lead to the stochastic equilibrium. In conclusion, our framework is quite flexible for many application scenarios and hence to be applicable for most transportation systems. As a supplementary material, the proposed framework is implemented in Python/C++ and open-sourced on Github[1].

References

Abdelghany, K. & Mahmassani, H. (2001), 'Dynamic trip assignment-simulation model for intermodal transportation networks', *Transportation Research Record: Journal of the Transportation Research Board* (1771), 52–60.

Abdulaal, M. & LeBlanc, L. J. (1979), 'Methods for combining modal split and equilibrium assignment models', *Transportation Science* **13**(4), 292–314.

Arnott, R., de Palma, A. & Lindsey, R. (1990), 'Departure time and route choice for the morning commute', *Transportation Research Part B: Methodological* **24**(3), 209–228.

Axhausen, K. W., Balmer, M., Meister, K., Rieser, M. & Nagel, K. (2008), 'Agent-based simulation of travel demand: Structure and computational performance of matsim-t', *Arbeitsbericht Verkehrs-und Raumplanung* **504**.

Axhausen, K. W., Polak, J., Boltze, M. & Puzicha, J. (1994), 'Effectiveness of the parking guidance information system in frankfurt am main', *Traffic Engineering+ Control* **35**(5), 304–9.

Chabini, I. (1998), 'Discrete dynamic shortest path problems in transportation applications: Complexity and algorithms with optimal run time', *Transportation Research Record: Journal of the Transportation Research Board* (1645), 170–175.

Chiabaut, N. (2015), 'Evaluation of a multimodal urban arterial: The passenger macroscopic fundamental diagram', *Transportation Research Part B: Methodological* **81**, 410–420.

Dafermos, S. (1982), 'The general multimodal network equilibrium problem with elastic demand', *Networks* **12**(1), 57–72.

Daganzo, C. F. (1994), 'The cell transmission model: a dynamic representation of highway traffic consistent with the hydrodynamic theory', *Transportation Research Part B* **28**, 269–287.

Daganzo, C. F. (1995), 'The cell transmission model, part II: Network traffic', *Transportation Research Part B* **29**, 79–93.

Facchinei, F. & Pang, J.-S. (2007), *Finite-dimensional variational inequalities and complementarity problems*, Springer Science & Business Media.

---

[1] https://github.com/Lemma1/Multimodal-DUE

Fernández, E., De Cea, J., Florian, M. & Cabrera, E. (1994), 'Network equilibrium models with combined modes', *Transportation Science* **28**(3), 182–192.

Florian, M. (1977), 'A traffic equilibrium model of travel by car and public transit modes', *Transportation Science* **11**(2), 166–179.

Florian, M. & Los, M. (1979), 'Determining intermediate origin-destination matrices for the analysis of composite mode trips', *Transportation Research Part B: Methodological* **13**(2), 91–103.

Florian, M. & Spiess, H. (1983), 'On binary mode choice/assignment models', *Transportation Science* **17**(1), 32–47.

Garcia, R. & Marin, A. (2005), 'Network equilibirum with combined modes: models and solution algorithms', *Transportation Research Part B* **39**, 223–254.

Han, D. & Lo, H. K. (2002), 'New alternating direction method for a class of nonlinear variational inequality problems', *Journal of optimization theory and applications* **112**(3), 549–560.

Horni, A., Nagel, K. & Axhausen, K. W. (2016), *The multi-agent transport simulation MATSim*, Ubiquity Press London:.

Huang, H.-J. & Lam, W. H. (2002), 'Modeling and solving the dynamic user equilibrium route and departure time choice problem in network with queues', *Transportation Research Part B: Methodological* **36**(3), 253–273.

Jin, W.-L. (2012), 'A link queue model of network traffic flow', *arXiv preprint arXiv:1209.2361* .

Lam, W. H. & Huang, H.-J. (1992), 'A combined trip distribution and assignment model for multiple user classes', *Transportation Research Part B* **26**(4), 273–287.

Lebacque, J. (1996), 'The godunov scheme and what it means for first order traffic flow models', *Procedings of International Symposium of Transport and Traffic Theory* pp. 79 – 102.

Leblanc, L. J. & Abdulaal, M. (1982), 'Combined mode split-assignment and distribution-model split-assignment models with multiple groups of travelers', *Transportation Science* **16**(4), 430–442.

Levin, M. W., Pool, M., Owens, T., Juri, N. R. & Waller, S. T. (2015), 'Improving the convergence of simulation-based dynamic traffic assignment methodologies', *Networks and Spatial Economics* **15**(3), 655–676.

Liu, H. X., Ding, L., Ban, J. X., Chen, A. & Chootinan, P. (2006), A streamlined network calibration procedure for california sr41 corridor traffic simulation study, *in* '85th Annual Meeting of the Transportation Research Board, Washington, DC'.

Liu, J. & Zhou, X. (2016), 'Capacitated transit service network design with boundedly rational agents', *Transportation Research Part B: Methodological* **93**, 225–250.

Liu, W. & Geroliminis, N. (2017), 'Doubly dynamics for multi-modal networks with park-and-ride and adaptive pricing', *Transportation Research Part B: Methodological* **102**, 162–179.

Lo, H. K. & Szeto, W. Y. (2002), 'A cell-based variational inequality formulation of the dynamic user optimal assignment problem', *Transportation Research Part B: Methodological* **36**(5), 421–443.

Lo, H. K., Yip, C.-W. & Wan, Q. K. (2004), 'Modeling competitive multi-modal transit services: a nested logit approach', *Transportation Research Part C: Emerging Technologies* **12**(3), 251–272.

Lo, H. K., Yip, C. & Wan, K. (2003), 'Modeling transfer and non-linear fare structure in multi-modal network', *Transportation Research Part B: Methodological* **37**(2), 149–170.

Ma, W., Pi, X. & Qian, S. (2019), 'Estimating multi-class dynamic origin-destination demand through a forward-backward algorithm on computational graphs', *arXiv preprint arXiv:1903.04681* .

Ma, W. & Qian, S. (2015), Traffic impact of the greenfield bridge closure. the public works of pittsburgh technical report, Technical report, Civil and Environmental Engineering, Carnegie Mellon University.

Ma, W. & Qian, Z. S. (2018), 'Estimating multi-year 24/7 origin-destination demand using high-granular multi-source traffic data', *Transportation Research Part C: Emerging Technologies* **96**, 96–121.

Meschini, L., Gentile, G. & Papola, N. (2007), A frequency based transit model for dynamic traffic assignment to multimodal networks, *in* 'Proceedings of 17th International Symposium on Transportation and Traffic Theory, London'.

Nagurney, A. (2009), 'Variational inequalities', *Encyclopedia of Optimization* pp. 3989–3994.

Nie, Y. (2006), A variational inequality approach for inferring dynamic origin-destination travel demands, PhD thesis, University of California, Davis.

Nie, Y. M. & Zhang, H. M. (2010), 'Solving the dynamic user optimal assignment problem considering queue spillback', *Networks and Spatial Economics* **10**(1), 49–71.

Nie, Y. & Zhang, H. (2007), 'Solving the dynamic user optimal assignment problem considering queue spillback', *Networks and Spatial Economics* **DOI:10.1007/s11067-007-9022-y**.

Patriksson, M. (2004), 'Sensitivity analysis of traffic equilibria', *Transportation Science* **38**(3), 258–281.

Pi, X., Egge, M., Whitmore, J., Silbermann, A. & Qian, Z. S. (2018), 'Understanding transit system performance using avl-apc data: An analytics platform with case studies for the pittsburgh region', *Journal of Public Transportation* **21**(2), 2.

Pi, X., Ma, W. & Qian, Z. S. (2019), Large-scale mesoscopic network modeling with cars and trucks: A case study in pittsburgh, Technical report.

Pi, X. & Qian, Z. S. (2017), 'A stochastic optimal control approach for real-time traffic routing considering demand uncertainties and travelers choice heterogeneity', *Transportation Research Part B: Methodological* **104**, 710–732.

PTV (2018), '*VISUM-VISSIM*'. http://vision-traffic.ptvgroup.com/en-us/products/ [Accessed: 01/31/2019].

Qian, Z. S., Li, J., Li, X., Zhang, M. & Wang, H. (2017), 'Modeling heterogeneous traffic flow: A pragmatic approach', *Transportation Research Part B: Methodological* **99**, 183–204.

Qian, Z. S. & Rajagopal, R. (2014), 'Optimal dynamic parking pricing for morning commute considering expected cruising time', *Transportation Research Part C: Emerging Technologies* **48**, 468–490.

Qian, Z. S., Xiao, F. E. & Zhang, H. (2012), 'Managing morning commute traffic with parking', *Transportation research part B: methodological* **46**(7), 894–916.

Qian, Z. S. & Zhang, H. M. (2011), 'Modeling multi-modal morning commute in a one-to-one corridor network', *Transportation Research Part C: Emerging Technologies* **19**(2), 254–269.

Sheffi, Y. (1985), *Urban transportation networks*, Vol. 6, Prentice-Hall, Englewood Cliffs, NJ.

Tobin, R. L. & Friesz, T. L. (1988), 'Sensitivity analysis for equilibrium network flow', *Transportation Science* **22**(4), 242–250.

Tong, L., Pan, Y., Shang, P., Guo, J., Xian, K. & Zhou, X. (2019), 'Open-source public transportation mobility simulation engine dtalite-s: A discretized space–time network-based modeling framework for bridging multi-agent simulation and optimization', *Urban Rail Transit* **5**(1), 1–16.

Van Lint, J., Hoogendoorn, S. & Schreuder, M. (2008), 'Fastlane: New multiclass first-order traffic flow model', *Transportation Research Record: Journal of the Transportation Research Board* (2088), 177–187.

Verbas, İ. Ö., Mahmassani, H. S. & Hyland, M. F. (2015), 'Dynamic assignment-simulation methodology for multimodal urban transit networks', *Transportation Research Record: Journal of the Transportation Research Board* (2498), 64–74.

Wie, B.-W., Tobin, R. L., Friesz, T. L. & Bernstein, D. (1995), 'A discrete time, nested cost operator approach to the dynamic network user equilibrium problem', *Transportation Science* **29**(1), 79–92.

Wigan, M. R. & Bamford, T. (1973), An equilibrium model of bus and car travel over a road network, Technical report.

Xu, S., Chen, X., Pi, X., Joe-Wong, C., Zhang, P. & Noh, H. Y. (2019*a*), 'ilocus: Incentivizing vehicle mobility to optimize sensing distribution in crowd sensing', *IEEE Transactions on Mobile Computing* pp. 1–1.

Xu, S., Chen, X., Pi, X., Joe-Wong, C., Zhang, P. & Noh, H. Y. (2019*b*), Vehicle dispatching for sensing coverage optimization in mobile crowdsensing systems, *in* 'Proceedings of the 18th International Conference on Information Processing in Sensor Networks', ACM, pp. 311–312.

Xu, S., Zhang, L., Zhang, P. & Noh, H. Y. (2016), An indirect traffic monitoring approach using building vibration sensing system, *in* 'Proceedings of the 14th ACM Conference on Embedded Network Sensor Systems CD-ROM', ACM, pp. 374–375.

Xu, S., Zhang, L., Zhang, P. & Noh, H. Y. (2017), 'An information-theoretic approach for indirect train traffic monitoring using building vibration', *Frontiers in Built Environment* **3**, 22.

Yang, S., Ma, W., Pi, X. & Qian, S. (2019), 'A deep learning approach to real-time parking occupancy prediction in spatio-termporal networks incorporating multiple spatio-temporal data sources', *arXiv preprint arXiv:1901.06758* .

Yang, S. & Qian, Z. S. (2017), 'Turning meter transactions data into occupancy and payment behavioral information for on-street parking', *Transportation Research Part C: Emerging Technologies* **78**, 165–182.

Zhang, K., Nair, R., Mahmassani, H. S., Miller-Hooks, E. D., Arcot, V. C., Kuo, A., Dong, J. & Lu, C.-C. (2008), 'Application and validation of dynamic freight simulation–assignment model to large-scale intermodal rail network: Pan-european case', *Transportation Research Record* **2066**(1), 9–20.

Zhang, M., Ma, J., Singh, S. P. & Chu, L. (2008), Developing calibration tools for microscopic traffic simulation final report part iii: Global calibration-od estimation, traffic signal enhancements and a case study, Technical report.

Zhang, P. & Qian, Z. S. (2018), 'User-centric interdependent urban systems: Using time-of-day electricity usage data to predict morning roadway congestion', *Transportation Research Part C: Emerging Technologies* **92**, 392–411.

Zheng, N. & Geroliminis, N. (2016), 'Modeling and optimization of multimodal urban networks with limited parking and dynamic pricing', *Transportation Research Part B: Methodological* **83**, 36–58.

Zheng, N., Rérat, G. & Geroliminis, N. (2016), 'Time-dependent area-based pricing for multimodal systems with heterogeneous users in an agent-based environment', *Transportation Research Part C: Emerging Technologies* **62**, 133–148.

Zhou, X., Mahmassani, H. S. & Zhang, K. (2008), 'Dynamic micro-assignment modeling approach for integrated multimodal urban corridor management', *Transportation Research Part C: Emerging Technologies* **16**(2), 167–186.

Zhou, X. & Taylor, J. (2014), 'Dtalite: A queue-based mesoscopic traffic simulator for fast model evaluation and calibration', *Cogent Engineering* **1**(1), 961345.

Zhu, D. & Marcotte, P. (1993), 'Modified descent methods for solving the monotone variational inequality problem', *Operations Research Letters* **14**(2), 111–120.

Appendix A. Notation Table

The main notations used in this paper are in Table A.4. Other notations not included in the table were introduced in the text.

Table A.4: The main notations used in this paper.

Notations	Description
t	index of time
r, s	indices of origins and destinations, respectively
m	index of first level mode choices
$g(m)$	index of second level mode choices
k	index of paths
$w_{k,t}^{rs}$	actual travel time through path k at time t from r to s, unit: second
$c_{m,k,t}^{rs}, c_{m,g(m),k,t}^{rs}$	generalized travel cost of path k in mode m and in mode $\{m, g(m)\}$ at time t from r to s, unit: dollar
$\mu_{m,t}^{rs}, \mu_{m,g(m),t}^{rs}$	equilibrium travel cost of mode m and $\{m, g(m)\}$ at time t from r to s, unit: dollar
P^{rs}	set of all paths from r to s
$P_m^{rs}, P_{m,g(m)}^{rs}$	set of paths of mode m and $\{m, g(m)\}$ from r to s
$f_{m,k,t}^{rs}, f_{m,g(m),k,t}^{rs}$	flow of path k in mode m and in mode $\{m, g(m)\}$ at time t from r to s
$h_{m,t}^{rs}, h_{m,g(m),t}^{rs}$	total flow of mode m and $\{m, g(m)\}$ at time t from r to s
q_t^{rs}	overall flow of all modes at time t from r to s
$\mathbf{f}$	vector of path flows
Λ_1, Λ_2	vectors of generalized costs
Ω_1, Ω_2	sets of feasible path flow assignments
δ_k^{rs}	transit fare of transit route k from r to s, unit: dollar
$\sigma_{k,t}^{rs}$	perceived inconvenience cost of the transit mode of transit route k from r to s, unit: dollar
p_i	parking fee at parking lot i, unit: dollar
ϵ_i	average parking time of parking lot i
E_i	total capacity of the parking lot i
$\Delta_{k,t}^{rs}(n)$	carpooling impedance cost through path k at time t from r to s with total n riders, unit: dollar
t^*	standard work starting time
α, γ, β	unit cost of travel time, for arriving late and for arriving early, respectively, unit: dollar/hour
$\alpha^m, \alpha_{g(m)}^m, \beta_1, \beta_2^m$	parameters in the nested-logit mode choice model